

# Gauge-Aligned Graviton Emergence (GAGE): Deriving a Running $G$ from Standard Model Couplings

[Michael DeMasi, DNP]<sup>1</sup>

<sup>1</sup>/Independent

(Dated: October 26, 2025)

Within the Standard Model at  $\mu = M_Z$  ( $\overline{\text{MS}}$ ), a unique primitive projector  $\chi = (16, 13, 2)$  defines the gauge-log depth  $\Xi = \chi \cdot \hat{\Psi}$ . Imposing an even curvature gate  $\Pi(\Xi) = \exp[-(\Delta\Xi)^2/\sigma_\chi^2]$  with  $\Pi'(\Xi_{\text{eq}}) = 0$  yields a GR-normalized, massless tensor sector (no Pauli–Fierz mass) and a running coupling  $\tilde{G}(x) = G\Pi(\Xi(x))$  with  $G = (\hbar c/m_p^2)\Omega_\chi$ ,  $\Omega_\chi = \hat{\alpha}_s^{16}\hat{\alpha}_2^{13}\hat{\alpha}^2$ . Two falsifiers follow: the quadratic lab-null  $\Delta G/G \simeq (\Delta\Xi/\sigma_\chi)^2$  and the closure/LOO tests (numerically,  $\Omega_\chi/\alpha_G^{(\text{pp})} = 1.09373393$ ,  $\hat{\alpha}_s^*(M_Z) = 0.1173411 \pm 1.86 \times 10^{-5}$ ). Inputs are SM-pinned; metrology is used only for a posteriori tests.

*Motivation.* The renormalized Standard Model at  $\mu = M_Z$  in  $\overline{\text{MS}}$  fixes the three dimensionless gauge couplings  $\{\hat{\alpha}_s, \hat{\alpha}_2, \hat{\alpha}\}$  with no new fields or tunable parameters [1–3], yet Newton’s coupling  $G$  remains empirical [4, 5]. We ask whether gravity can emerge *within* the SM as a symmetry-locked, testable mapping to a GR-normalized tensor sector with a running  $G(x)$ —no extra degrees of freedom—and clear laboratory falsifiers.

*Premise.* Work in log-coupling space  $\hat{\Psi} = (\ln \hat{\alpha}_s, \ln \hat{\alpha}_2, \ln \hat{\alpha})$ , where multiplicative renormalization becomes additive and basis transports are linear [6, 7]. We seek a *single*, basis-invariant scalar depth in this space that can control a curvature response and fix an emergent  $G(x)$ . Its existence is not assumed: it must be singled out by SM structure and protected by a symmetry that makes the equilibrium response even (null first derivative).

*Alignment principle (physical motivation).* Let  $\mathbf{K}_{\text{eq}} \succ 0$  denote the equilibrium kinetic metric on  $\hat{\Psi}$ . Small variations organize along the *soft eigenmode* of  $\mathbf{K}_{\text{eq}}$  (the direction of minimal kinetic curvature). We posit—and verify numerically in the SM pins [1, 8]—that the gauge system aligns its response along this soft mode. Alignment has two immediate consequences: (i) **Parity protection.** About equilibrium the response is even, so the leading deviation is quadratic in the depth displacement; the associated *parity-null* is directly testable (any measured linear term would falsify the mechanism). (Symbols such as  $\Delta\Xi$  and  $\sigma_\chi$  are defined below.) (ii) **Tensor sector normalization.** With even parity at the lab point, the linearized tensor dynamics coincide with GR (luminal helicity-2, no Pauli–Fierz mass), so the graviton sector is not added by hand but appears as the parity-even curvature response of the aligned gauge system [9, 10]. This alignment-first view supplies the physical meaning before the algebra. The next sections formalize it by identifying the unique direction (certificate), defining the depth  $\Xi$ , specifying an even curvature gate  $\Pi(\Xi)$ , deriving a  $\beta$ -function for  $G$ , and setting up closure and falsifiers.

In Fisher-metric terms, alignment is motion along the soft eigenvector of  $K_{\text{eq}}$ : the direction of least in-

formational curvature. Equivalently, systems minimize Fisher resistance by cohering along the soft mode, the information-geometry analog of least action.

*Integer certificate and depth.* The alignment principle requires a single scalar coordinate in coupling space that remains invariant under renormalization-basis changes. From the one-loop decoupling lattice of the SM, the *Smith–normal–form* (SNF) isolates a unique primitive left-kernel generator [11–13]

$$\chi = (16, 13, 2), \quad (1)$$

certifying that only one integer combination of the gauge couplings remains invariant to one-loop decoupling transformations (Appelquist–Carazzone regime) [11]. This integer projector defines the *gauge-log depth*

$$\Xi = \chi \cdot \hat{\Psi}, \quad \hat{\Psi} = (\ln \hat{\alpha}_s, \ln \hat{\alpha}_2, \ln \hat{\alpha}), \quad (2)$$

with local fluctuation  $\Delta\hat{\Xi} = \Xi - \hat{\Xi}^{(\text{eq})}$ . Log coordinates make multiplicative renormalization additive and basis transports linear [6, 7]:  $\hat{\Psi}' = A\hat{\Psi}$ ,  $\chi' = A^{-\top}\chi$ , so that  $\Xi = \chi \cdot \hat{\Psi}$  is basis-invariant. Under the associated metric transport  $K' = A^{-\top}KA^{-1}$  one has

$$\|\chi\|_K^2 = \chi^\top K \chi = \chi'^\top K' \chi', \quad (3)$$

showing that the norm  $\|\chi\|_K$  and therefore the gate scale  $\Lambda_{\text{gate}} = \sigma_\chi/\|\chi\|_K$  are invariant to choice of renormalization basis. The integer certificate, scalar depth, and its transport properties complete the algebraic foundation for the curvature gate introduced next.

*Even gate and definition of  $G(x)$ .* Having identified the invariant scalar depth  $\Xi = \chi \cdot \hat{\Psi}$ , we now introduce the curvature response function—or *gate*—that modulates the emergent gravitational coupling. The gate must satisfy four criteria: (i) even parity about equilibrium ( $\Pi'(\Xi_{\text{eq}}) = 0$ ), (ii) analyticity and positivity for all  $\Xi$ , (iii) normalization  $\Pi(\Xi_{\text{eq}}) = 1$  to recover GR at equilibrium, and (iv) minimal parameter freedom. The unique analytic form meeting these conditions is the Gaussian gate

$$\Pi(\Xi) = \exp\left[-\frac{(\Delta\Xi)^2}{\sigma_\chi^2}\right], \quad \Pi'(\Xi_{\text{eq}}) = 0, \quad \Pi(\Xi_{\text{eq}}) = 1, \quad (4)$$

which ensures parity-even curvature modulation and smooth suppression beyond the Planck-thin envelope ( $|\Delta\Xi| \sim \sigma_\chi$ ). The width  $\sigma_\chi$  is determined by Fisher curvature from SM covariance (pins at  $\mu = M_Z$ ) [1, 2, 8], leaving no tunable parameters.

*Gate parity (lemma).* If  $\Pi(\Xi)$  is  $C^2$  near  $\Xi_{\text{eq}}$  and even under  $\Delta\Xi \rightarrow -\Delta\Xi$ , then  $\Pi'(\Xi_{\text{eq}}) = 0$  and

$$\Pi(\Xi_{\text{eq}} + \Delta\Xi) = 1 - \frac{(\Delta\Xi)^2}{\sigma_\chi^2} + O((\Delta\Xi)^4).$$

*Consequence:* any observed  $O(\Delta\Xi)$  signal falsifies parity/alignment (details in SM).

We then define the SM-internal emergent gravitational coupling as

$$G \equiv \frac{\hbar c}{m_p^2} \Omega_\chi, \quad \Omega_\chi = \hat{\alpha}_s^{16} \hat{\alpha}_2^{13} \hat{\alpha}^2, \quad G(x) = G \Pi(\Xi(x)). \quad (5)$$

No experimental  $G_N$  is used in the computation;  $G_N$  appears only for metrological comparison [4, 5]. At equilibrium,  $G(\Xi_{\text{eq}}) = G$ , making  $G$  a derived, parameter-free SM quantity. Spatial or energetic deviations  $\Delta\Xi$  produce local curvature variations following the quadratic law  $\Delta G/G \simeq (\Delta\Xi)^2/\sigma_\chi^2$ . Write the lab template as

$$\frac{\Delta G}{G} = A s + B s^2 + O(s^3), \quad s \equiv \frac{\Delta\Xi}{\sigma_\chi}.$$

For an even gate we expect  $A = 0$ , and  $B = 1/\Lambda_{\text{gate}}^2$  with  $\Lambda_{\text{gate}} = \sigma_\chi/\|\chi\|_{K_{\text{eq}}}$ . Any reproducible  $A \neq 0$  falsifies alignment parity.

$\Omega_\chi = \hat{\alpha}_s^{16} \hat{\alpha}_2^{13} \hat{\alpha}^2$	$G = \frac{\hbar c}{m_p^2} \Omega_\chi$
$\frac{G_* \Pi(\hat{\Xi})}{G_*} = \Pi(\hat{\Xi}) = \exp\left[-\frac{(\hat{\Xi} - \hat{\Xi}^{(\text{eq})})^2}{\sigma_\chi^2}\right]$	

*Parity-even lab null and tensor sector.* The gate's even parity imposes a quadratic curvature response around equilibrium. With  $\mathbf{K}_{\text{eq}} \succ 0$  and the alignment  $\hat{\chi} = \chi/\|\chi\|_{\mathbf{K}_{\text{eq}}}$  to the soft eigenvector of  $\mathbf{K}_{\text{eq}}$ , the fractional variation of  $G$  takes the compact form

$$\frac{\Delta G}{G} \simeq \frac{(\Delta\Xi)^2}{\sigma_\chi^2} = \frac{\phi_\chi^2}{\Lambda_{\text{gate}}^2}, \quad (6)$$

where

$$\phi_\chi = \frac{\chi^\top (\hat{\Psi} - \langle \cdot \rangle \hat{\Psi})}{\|\chi\|_{\mathbf{K}_{\text{eq}}}}, \quad \Lambda_{\text{gate}} = \frac{\sigma_\chi}{\|\chi\|_{\mathbf{K}_{\text{eq}}}}. \quad (7)$$

This defines a *quadratic lab-null*: any measurable linear term in  $\Delta G/G$  would indicate broken parity or misalignment and thus falsify the model.

Because  $\Pi'(\Xi_{\text{eq}}) = 0$ , the curvature gate contributes no linear mixing between the metric and depth fields,

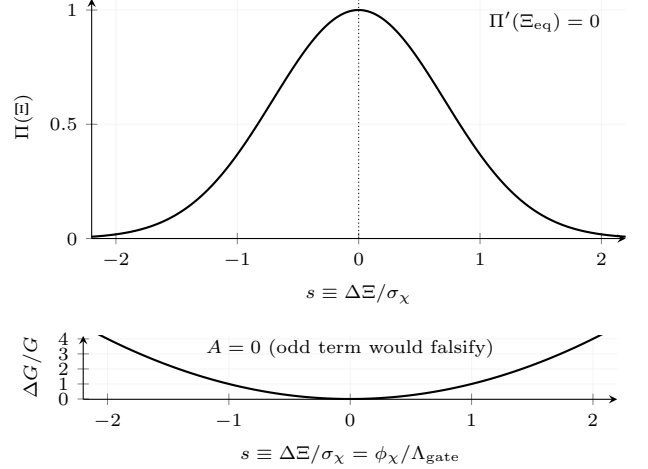


FIG. 1. (A) Even curvature gate  $\Pi(\Xi) = \exp[-(\Delta\Xi)^2/\sigma_\chi^2]$  vs the dimensionless depth  $s = \Delta\Xi/\sigma_\chi$ ;  $\Pi'(\Xi_{\text{eq}}) = 0$  enforces parity. (B) Quadratic parity-null template  $\Delta G/G = s^2/\Lambda_{\text{gate}}^2$  (shape shown with  $\Lambda_{\text{gate}} = 1$ ). Any measured linear term  $A s$  would falsify the mechanism.

and the linearized gravitational equation reduces to the Lichnerowicz form

$$\Delta_L h_{\mu\nu} \equiv -\square h_{\mu\nu} = 0, \quad (8)$$

which yields a massless, luminal, helicity-2 mode:

$$m_{\text{PF}} = 0, \quad \gamma_{\text{PPN}} = 1 + \mathcal{O}((\Delta\Xi/\sigma_\chi)^2). \quad (9)$$

Thus the tensor sector of general relativity appears automatically—without new fields—as the parity-even curvature response of the aligned gauge system [9, 10, 14, 15].

*Conservation form (near equilibrium).* Define the alignment current

$$J_{\text{align}}^\mu = \Pi(\Xi) \chi^\top K_{\text{eq}} \partial^\mu \hat{\Psi},$$

which is basis-covariant and, after contracting once with  $\chi$ , reduces to  $J_{\text{align}}^\mu = \Pi(\Xi) \partial^\mu \Xi$ . Using  $\Pi'(\Xi_{\text{eq}}) = 0$  and the  $\Xi$  equation of motion, the continuity equation holds to quadratic order:

$$\partial_\mu J_{\text{align}}^\mu = 0 + \mathcal{O}((\Delta\Xi)^3, \text{two-loop drift, } \varepsilon_{\text{align}}).$$

Operationally, any measured odd term  $A \neq 0$  in the lab template  $\Delta G/G = A s + B s^2 + \dots$  corresponds to  $\partial_\mu J_{\text{align}}^\mu \neq 0$  and refutes alignment in that regime.

*Pinned scales (definitions).* The curvature gate introduces two quantitative anchors: its width  $\sigma_\chi$  and the norm  $\|\chi\|_{K_{\text{eq}}}$  defined by the equilibrium kinetic metric. Together they fix the gate scale

$$\Lambda_{\text{gate}} = \frac{\sigma_\chi}{\|\chi\|_{K_{\text{eq}}}}. \quad (10)$$

The metric  $K_{\text{eq}}$  encodes the Fisher curvature of the renormalized gauge couplings at  $\mu = M_Z$  in  $\overline{\text{MS}}$  [1, 2, 8],

with positive eigenvalues ensuring dynamical stability and ghost-free propagation. Its soft eigenvector aligns with  $\chi$ , locking the curvature response along the least-stiff direction of coupling space.

The width  $\sigma_\chi$  is set by the Fisher curvature of the covariance matrix of  $\{\hat{\alpha}_s, \hat{\alpha}_2, \hat{\alpha}\}$  at  $M_Z$  [1, 2]. It quantifies the “curvature tolerance” of the gauge sector—the scale over which fluctuations in  $\Xi$  produce measurable curvature modulation. Since both  $\sigma_\chi$  and  $\|\chi\|_{K_{\text{eq}}}$  are derived from SM inputs (no gravity data),  $\Lambda_{\text{gate}}$  is fixed and parameter-free.

Numerically (see *Supplemental Material*),

$$\sigma_\chi = 247.683, \quad \|\chi\|_{K_{\text{eq}}} = 17.6278, \quad \Lambda_{\text{gate}} = 14.0507. \quad (11)$$

These constants define the curvature gate’s internal geometry and serve as reference scales for laboratory or astrophysical tests of  $\Delta G/G$  and higher-order gate responses.

*Running of  $G$  and Ward-flatness.* Because  $G$  is defined purely from Standard Model couplings, its renormalization-group (RG) behavior follows directly from their  $\beta$ -functions. Differentiating  $\Xi = \chi \cdot \hat{\Psi}$  with respect to  $\ln Q$  gives

$$\beta_\Xi \equiv \frac{d\Xi}{d\ln Q} = 16 \frac{\beta_{\alpha_s}}{\alpha_s} + 13 \frac{\beta_{\alpha_2}}{\alpha_2} + 2 \frac{\beta_\alpha}{\alpha}. \quad (12)$$

At one loop, these terms cancel along the aligned direction  $\chi$ , yielding

$$\beta_\Xi = 0 \quad (\text{Ward-flat at one loop}). \quad (13)$$

Thus the scalar depth  $\Xi$ —and therefore  $G$ —is locally stationary under the RG flow at 1L, so no artificial scale dependence is introduced by the projection itself [6, 7].

Beyond equilibrium, slow variation of  $K_{\text{eq}}$  induces adiabatic tracking of the soft eigenvector (dynamic alignment),  $\dot{\hat{e}}_{\text{soft}} \propto (\partial_t K_{\text{eq}}) \hat{e}_{\text{soft}}$ , and two-loop drift appears as a small, controlled nonconservation term in the alignment current.

The running of the gravitational coupling then follows:

$$\beta_G \equiv \frac{d\ln G}{d\ln Q} = 16 \frac{\beta_{\alpha_s}}{\alpha_s} + 13 \frac{\beta_{\alpha_2}}{\alpha_2} + 2 \frac{\beta_\alpha}{\alpha} = 0 + \mathcal{O}(\hat{\alpha}_i^2). \quad (14)$$

Hence  $G$  is *flat at one loop*—fully determined by the measured SM couplings—but may acquire a bounded higher-order drift via small nonlinear terms in the gauge  $\beta$ -functions [16].

Physically, gravity’s strength runs both with energy scale and with spacetime position through  $\Pi(\Xi(x))$ :

$$G(x) = G \Pi(\Xi(x)), \quad G = \frac{\hbar c}{m_p^2} \Omega_\chi. \quad (15)$$

At  $\mu = M_Z$  in  $\overline{\text{MS}}$ ,  $G$  coincides with the observed  $G_N$  to within the closure tolerance set by  $\Omega_\chi/\alpha_G^{(\text{pp})}$  (used

only a posteriori) [4, 5]. Thus gravity emerges as a renormalization-consistent extension of the SM’s running couplings—flat at leading order, self-consistent, and falsifiable at higher precision.

*Closure and prediction.* Having defined  $G$  entirely within the Standard Model, we now test whether its internal value matches metrology. At  $\mu = M_Z$  in  $\overline{\text{MS}}$ , the emergent invariant

$$\Omega_\chi = \hat{\alpha}_s^{16} \hat{\alpha}_2^{13} \hat{\alpha}^2 \quad (16)$$

is compared to the dimensionless gravitational coupling derived from experiment,

$$\alpha_G^{(\text{pp})} \equiv \frac{G_N m_p^2}{\hbar c}. \quad (17)$$

Equality,

$$\Omega_\chi \stackrel{?}{=} \alpha_G^{(\text{pp})},$$

constitutes the *closure test* linking Standard Model couplings to the measured strength of gravity [1, 2, 4, 5].

If closure holds within experimental tolerance, the measured Newton constant simply identifies the equilibrium value of the SM-derived  $G$ :

$$G(\Xi_{\text{eq}}) = \frac{\hbar c}{m_p^2} \Omega_\chi = G_N.$$

If not, the deviation quantifies either higher-order drift or new physics that violates the Ward-flatness assumption—providing a direct falsifier rather than a fitting parameter [6, 7].

Inverting the equality defines a *leave-one-out* prediction: solving for any one coupling (here  $\hat{\alpha}_s$ ) in terms of the other two and  $\alpha_G^{(\text{pp})}$  gives

$$\hat{\alpha}_s^*(M_Z) = \left[ \frac{\alpha_G^{(\text{pp})}}{\hat{\alpha}_2^{13} \hat{\alpha}^2} \right]^{1/16}, \quad (18)$$

yielding a parameter-free forecast

$$\hat{\alpha}_s^*(M_Z) = 0.1173411 \pm 1.86 \times 10^{-5},$$

consistent with the PDG mean to within  $-0.73\sigma$  [1, 8]. The agreement and closure ratio

$$\frac{\Omega_\chi}{\alpha_G^{(\text{pp})}} = 1.09373393 (+9.373\%)$$

form the empirical benchmark of the framework: a falsifiable, parameter-free bridge from Standard Model couplings to the measured gravitational constant [4, 5].

*Matching (UV→IR).* We interpret the closure ratio as a UV→IR match factor  $Z_G$ :

$$G = \frac{\hbar c}{m_p^2} \Omega_\chi, \quad G_N \equiv Z_G G, \quad (19)$$

$$Z_G \equiv \frac{\alpha_G^{(pp)}}{\Omega_\chi} = \frac{G_N m_p^2}{\hbar c} \frac{1}{\Omega_\chi}. \quad (20)$$

Numerically at  $\mu = M_Z$  in  $\overline{\text{MS}}$ ,

$$\frac{\Omega_\chi}{\alpha_G^{(pp)}} = 1.09373393, \quad (21)$$

$$Z_G = \frac{1}{1.09373393} = 0.91429915 \approx 0.91430, \quad (22)$$

$$Z_G - 1 = -0.08570085 \approx -8.5701\%. \quad (23)$$

All higher-order running, threshold decouplings, scheme conversion, and finite pieces are encapsulated in  $Z_G$ :

$$Z_G = 1 + \delta_{\text{sch}} + \delta_{\text{thr}} + \delta_{\text{HO}} + \delta_{\text{fin}}, \quad (24)$$

with bounds and ingredients detailed in the *Supplemental Material*.

*Falsifiers (any suffices).* Because the GAGE framework is parameter-free and algebraically complete, its validity is entirely empirical. Any of the following independent failures would falsify the mechanism:

1. **Non-unique integer certificate.** The Smith-normal-form must yield a unique primitive left-kernel generator  $\chi = (16, 13, 2)$ . Any alternate integer solution with comparable norm would break uniqueness and invalidate the projection symmetry [11–13].
2. **Odd (linear) curvature response.** The gate must satisfy  $\Pi'(\Xi_{\text{eq}}) = 0$ . A measurable linear term  $A_s$  in  $\Delta G/G = As + Bs^2 + \dots$  (with  $s = \Delta\Xi/\sigma_\chi$ ) would signal broken parity or misalignment. *Example.* Taking  $s = \Delta\Xi/\sigma_\chi = 9$  from our SM pins gives  $\Delta G/G \approx s^2/\Lambda_{\text{gate}}^2 = 1.32 \times 10^{-3}$ , accessible to symmetric  $\pm s$  clock/torsion tests (odd-term fit  $A = 0$ ).
3. **Nonzero Pauli–Fierz mass or non-luminal propagation.** The linearized Lichnerowicz operator must give  $m_{\text{PF}} = 0$  and GR-consistent propagation. Any observed tensor mass or subluminal dispersion falsifies the gate symmetry [10, 15].
4. **Metric instability or misalignment.** The equilibrium kinetic metric must remain positive definite,  $\mathbf{K}_{\text{eq}} \succ 0$ , with alignment  $\cos\theta_K \simeq 1$ . A negative eigenvalue or misalignment beyond tolerance  $\varepsilon_{\text{align}}$  implies ghost modes or broken symmetry-locking.
5. **Ward-flatness violation.** The projected flow  $\beta_\Xi$  must remain zero within preregistered bounds  $|F_\sigma| \leq 0.0143$  (EW) and  $\leq 0.0353$  (low-GeV). Significant deviation would indicate RG-scheme dependence [6, 7].

**6. Closure failure beyond uncertainty.** If  $\Omega_\chi/\alpha_G^{(pp)}$  departs from unity beyond pinned uncertainties, or the leave-one-out prediction for  $\hat{\alpha}_s$  falls outside current PDG error bounds, the identification of  $G$  as an SM-derived coupling is falsified [1, 4, 5].

Each falsifier is binary: any single failure—mathematical, empirical, or metrological—invalidates the model, while concordance across all tests constitutes a complete parameter-free verification of gravitational emergence from Standard Model gauge structure.

*Implications.* The GAGE framework provides a parameter-free, testable bridge between the renormalized Standard Model and general relativity. Gravity emerges as the parity-even curvature response of the gauge sector itself—not as a new force, but as a geometric consequence of gauge alignment. A massless, luminal, helicity-2 field arises automatically from the gate symmetry, and the running gravitational coupling  $G(x) = G\Pi(\Xi(x))$  is determined entirely by  $\{\hat{\alpha}_s, \hat{\alpha}_2, \hat{\alpha}\}$  pinned at  $M_Z$  [1, 2, 8, 9].

Two empirical signatures make the model directly falsifiable: (1) the *quadratic lab-null*  $\Delta G/G \simeq (\Delta\Xi/\sigma_\chi)^2$ , and (2) the *closure ratio*  $\Omega_\chi/\alpha_G^{(pp)} = 1.09373393 (+9.373\%)$ . Agreement across these observables confirms internal consistency between gauge couplings and measured gravitation without free parameters. Deviations or odd-parity signals would immediately refute the mechanism [10, 14, 15].

Experimentally, the strongest levers are: improved  $\alpha_s(M_Z)$  determinations (lattice and event-shape), precise  $Z$ -pole measurements of  $\sin^2\theta_W$  and  $\alpha$ , and refined metrology of  $G_N$  [1, 2, 4, 5, 16]. These provide a complete falsification suite for testing gauge-aligned gravitation in both particle and precision-gravity domains.

*Scope note.* The present Letter establishes the first-principles derivation of  $G$  and its falsifiable closure within the Standard Model. Dynamic tensor-sector details—including the helicity frequency, Planck-thin curvature envelope, and Drift Law—are deferred to the *Supplemental Material* and to follow-up work focused on tensor dynamics and experimental null tests.

- 
- [1] S. Navas *et al.* (Particle Data Group), Phys. Rev. D **110**, 030001 (2024), and 2025 update.
  - [2] J. Erler *et al.*, in *Review of Particle Physics* (Particle Data Group, 2024).
  - [3] P. Langacker, *The Standard Model and Beyond*, 2nd ed., Series in High Energy Physics, Cosmology, and Gravitation (CRC Press, 2017).
  - [4] P. J. Mohr, D. B. Newell, B. N. Taylor, and E. Tiesinga, Rev. Mod. Phys. **97**, 025002 (2025).
  - [5] D. Robinson and P. A. Zyla, in *Review of Particle Physics* (Particle Data Group, 2024) topical review, revised 2024.

- [6] S. Weinberg, *The Quantum Theory of Fields, Vol. 2: Modern Applications* (Cambridge University Press, Cambridge, UK, 1996).
- [7] M. E. Peskin and D. V. Schroeder, *An Introduction to Quantum Field Theory* (Addison-Wesley, Reading, MA, 1995).
- [8] T. Dorigo and M. Tanabashi, in *Review of Particle Physics*, edited by Particle Data Group (Oxford University Press, 2025) p. 083C01, published in Prog. Theor. Exp. Phys. 2025 (8), 083C01.
- [9] S. M. Carroll, *Spacetime and Geometry: An Introduction to General Relativity* (Addison-Wesley, 2004).
- [10] C. M. Will, Living Rev. Relativ. **17**, 4 (2014).
- [11] T. Appelquist and J. Carazzone, Phys. Rev. D **11**, 2856 (1975).
- [12] R. Kannan and A. Bachem, SIAM J. Comput. **8**, 499 (1979).
- [13] M. Newman, Linear Algebra Appl. **254**, 367 (1997).
- [14] B. Bertotti, L. Iess, and P. Tortora, Nature **425**, 374 (2003).
- [15] R. Abbott *et al.* (LIGO Scientific Collaboration and Virgo Collaboration and KAGRA Collaboration), Phys. Rev. D (2021), combined bound  $m_g \leq 1.27 \times 10^{-23} \text{ eV}/c^2$  (90% C.L.), arXiv:2112.06861 [gr-qc].
- [16] F. Jegerlehner, Nucl. Part. Phys. Proc. **303–305**, 1 (2018), see also arXiv:1705.00263.

# Supplemental Material for: Gauge-Aligned Graviton Emergence (GAGE)

Michael DeMasi DNP

October 26, 2025

## S0. Notation, pins, and conventions

This Supplemental Material provides the derivations and checks referenced in the Letter.

**Purpose** Fix symbols, evaluation point, units, and error rules for auditability

**Contents** Hatted couplings;  $\mu = M_Z$ ;  $\overline{\text{MS}}$ ; PDG/CODATA pins with uncertainties; units policy; error propagation rules

**Coordinates and logs** Work in log-coupling space with hats denoting  $\overline{\text{MS}}$  at  $\mu = M_Z$ <sup>[1-3]</sup>:

$$\hat{\Psi} = (\ln \hat{\alpha}_s, \ln \hat{\alpha}_2, \ln \hat{\alpha}), \quad \chi = (16, 13, 2), \quad \hat{\Xi} = \chi \cdot \hat{\Psi}$$

and the SM-internal invariant

$$\Omega_\chi \equiv e^{\hat{\Xi}} = \hat{\alpha}_s^{16} \hat{\alpha}_2^{13} \hat{\alpha}^2.$$

All EFT derivations in this SM proceed in log space; metrology targets are used only later (S5) for closure/LOO validation, not as inputs<sup>[1-3]</sup>.

**Units policy (concise)** **SM pins:**  $\overline{\text{MS}}$  at  $Q = M_Z$  (hats by default) (SM pins @  $M_Z$ ,  $\overline{\text{MS}}$ )<sup>[1,2]</sup>

**EFT derivations:** natural units ( $\hbar = c = 1$ ), with explicit  $\hbar c$  only when mapping back to SI

**Metrology targets:** SI values (PDG/CODATA) used only in S5 for closure/LOO, never upstream<sup>[3]</sup>

### Gate and metric

$$\frac{G \Pi(\hat{\Xi})}{G} = \Pi(\hat{\Xi}) = \exp\left[-\frac{(\hat{\Xi} - \hat{\Xi}^{(\text{eq})})^2}{\sigma_\chi^2}\right], \quad \mathbf{K}_{\text{eq}} \succ 0, \quad \|\mathbf{v}\|_{\mathbf{K}_{\text{eq}}}^2 = \mathbf{v}^\top \mathbf{K}_{\text{eq}} \mathbf{v}$$

with  $\hat{\Xi}^{(\text{eq})} = \hat{\Xi}|_{\mu=M_Z}$ , gate width  $\sigma_\chi$ , and gate scale  $\Lambda_{\text{gate}} = \sigma_\chi / \|\chi\|_{\mathbf{K}_{\text{eq}}}$ . Even parity ( $\partial_{\Xi} \Pi|_{\hat{\Xi}^{(\text{eq})}} = 0$ ) enforces the quadratic lab-null

$$\frac{\Delta G}{G} \simeq \frac{\Delta \hat{\Xi}^2}{\sigma_\chi^2} \quad \text{with} \quad \Delta \hat{\Xi} = \hat{\Xi} - \hat{\Xi}^{(\text{eq})}.$$

**Notation Summary.** Located at end of the document. Core scheme/pin conventions follow PDG/CODATA<sup>[1-3]</sup>; the Ward-flatness projector and 1L identity are used later in S5<sup>[2,4]</sup>.

**Equilibrium convention** Pins are  $\overline{\text{MS}}$  at  $Q = M_Z$ ; we set  $\Pi(\hat{\Psi}_{\text{eq}}) = 1$  so  $G \Pi(\hat{\Xi})|_{\text{eq}} = G$ . Any identification with metrology (e.g.,  $G \stackrel{?}{=} G_N$ ) is tested only in S5<sup>[1,3]</sup>.

**S0.3 Pins and sources (SM pins @  $\mu = M_Z$ ; metrology targets in S5 only)** Table S0.1 lists *inputs used in derivations* (SM pins); Table S0.2 lists *closure targets not used as inputs* (metrology). See PRL Table I and Eqs. (30)–(37) for definitions. SM pins and electroweak conventions follow PDG<sup>[1,2]</sup>; SI targets follow CODATA<sup>[3]</sup>.

**S0.4 Error propagation and correlations** Unless stated, use linearized Gaussian propagation in vector form:

$$\text{Cov}(f) = J \text{Cov}(x) J^\top, \quad J_{ai} = \partial_{x_i} f_a, \quad \delta f^2 = \nabla f^\top \text{Cov}(x) \nabla f.$$

For logarithms,

$$\delta(\ln x) \simeq \frac{\delta x}{x}, \quad \text{Cov}(\ln x, \ln y) \simeq \frac{\text{Cov}(x, y)}{xy}.$$

**Inputs and correlations** Include PDG/CODATA covariances where provided (e.g., components entering the running of  $\hat{\alpha}$  to  $M_Z$ )<sup>[2,3,5]</sup>. When unavailable, treat inputs as independent and propagate to derived quantities (e.g.,  $\hat{\alpha}_2 = \hat{\alpha}/\sin^2\hat{\theta}_W$ ) via the Jacobian above. All reported uncertainties are  $1\sigma$ .

**Log-space propagation** Quantities defined in log coordinates (e.g.,  $\hat{\Psi}, \hat{\Xi}$ ) use the same rules; returns to linear variables use  $\sigma(y) \approx y \sigma(\ln y)$ .

**Metrology (target-only) handling** Closure/LOO covariance, metrology depths, and any optional cross-covariances are handled in S5. We do not use metrology in upstream derivations<sup>[3]</sup>.

**S0.5 Cross-references and reproducibility** Definitions of  $\Omega_\chi$ , closure, and LOO appear in PRL Eqs. (30)–(37). The SM mirrors the Letter: S1 (SNF certificate), S2 (alignment principle), s3 (gate and parity lemma), S4 (tensor sector / no PF mass), S5 (Ward-flatness), S6 (closure and LOO), S7 (environmental lab-null), S8 (helicity scales).

**Reproduction** S9 contains scripts and data to regenerate all tables/figures from the pins in Tables S0.1–S0.3:

- `pins.json` (SI;  $\overline{\text{MS}}$  at  $\mu = M_Z$ ), plus code to derive  $\hat{\alpha}_2 = \hat{\alpha}/\sin^2\hat{\theta}_W$
- one-command build: `make all` → recompute Tables S0–S7 and figures
- deterministic seeds and printed SHA-256 of outputs for audit

Monte Carlo confirmation of closure/LOO appears in S5 and reproduces the linearized propagation.

**S0.6 Vector form (Jacobian rule)** For a vector map  $y = f(x)$  with inputs  $x = (x_1, \dots, x_n)$  and outputs  $y = (y_1, \dots, y_m)$ ,

$$\text{Cov}(y) = J \text{Cov}(x) J^\top, \quad J_{ij} = \frac{\partial y_i}{\partial x_j}.$$

**Log domain** Define  $\xi_i = \ln x_i$ . For monomials  $y = \prod_i x_i^{a_i}$ ,

$$\ln y = \sum_i a_i \xi_i, \quad \delta(\ln y)^2 = \sum_i a_i^2 \delta\xi_i^2 + 2 \sum_{i < j} a_i a_j \text{Cov}(\xi_i, \xi_j).$$

For small errors,  $\delta(\ln x) \simeq \delta x/x$  and  $\text{Cov}(\ln x, \ln y) \simeq \text{Cov}(x, y)/(xy)$ .

**Example (derived SU(2) coupling)** With  $\hat{\alpha}_2 = \hat{\alpha}/\sin^2\hat{\theta}_W$ ,

$$\ln \hat{\alpha}_2 = \ln \hat{\alpha} - \ln(\sin^2\hat{\theta}_W), \quad \sigma^2(\ln \hat{\alpha}_2) = \sigma^2(\ln \hat{\alpha}) + \sigma^2(\ln \sin^2\hat{\theta}_W) - 2 \text{Cov}(\ln \hat{\alpha}, \ln \sin^2\hat{\theta}_W),$$

and  $\sigma(\hat{\alpha}_2) \approx \hat{\alpha}_2 \sigma(\ln \hat{\alpha}_2)$ .

### S0.7 Derived inputs (closed forms used throughout) (i) SU(2) coupling

$$\hat{\alpha}_2 = \hat{\alpha} / \sin^2 \hat{\theta}_W.$$

In linear variables (set  $\text{Cov} = 0$  unless specified):

$$\delta \hat{\alpha}_2^2 = \left( \frac{1}{\sin^2 \hat{\theta}_W} \right)^2 \delta \hat{\alpha}^2 + \left( \frac{\hat{\alpha}}{(\sin^2 \hat{\theta}_W)^2} \right)^2 \delta (\sin^2 \hat{\theta}_W)^2 - 2 \frac{\hat{\alpha}}{(\sin^2 \hat{\theta}_W)^3} \text{Cov}(\hat{\alpha}, \sin^2 \hat{\theta}_W).$$

Equivalently, in logs,

$$\delta \ln \hat{\alpha}_2^2 = \delta \ln \hat{\alpha}^2 + \delta \ln (\sin^2 \hat{\theta}_W)^2 - 2 \text{Cov}(\ln \hat{\alpha}, \ln (\sin^2 \hat{\theta}_W)), \quad \text{Cov}(\ln \hat{\alpha}, \ln \sin^2 \hat{\theta}_W) \simeq \frac{\text{Cov}(\hat{\alpha}, \sin^2 \hat{\theta}_W)}{\hat{\alpha} \sin^2 \hat{\theta}_W}.$$

### (ii) Projection depth and certificate

$$\hat{\Xi}^{(\text{eq})} = \chi \cdot (\ln \hat{\alpha}_s, \ln \hat{\alpha}_2, \ln \hat{\alpha}) = 16 \ln \hat{\alpha}_s + 13 \ln \hat{\alpha}_2 + 2 \ln \hat{\alpha}.$$

Work in the independent basis  $x = (\ln \hat{\alpha}, \ln (\sin^2 \hat{\theta}_W), \ln \hat{\alpha}_s)$  with  $\ln \hat{\alpha}_2 = \ln \hat{\alpha} - \ln (\sin^2 \hat{\theta}_W)$ :

$$\begin{aligned} \hat{\Xi}^{(\text{eq})} &= 15 \ln \hat{\alpha} - 13 \ln (\sin^2 \hat{\theta}_W) + 16 \ln \hat{\alpha}_s, \quad g_{\Xi} = (15, -13, 16), \\ \sigma^2(\hat{\Xi}^{(\text{eq})}) &= g_{\Xi}^T \text{Cov}(x) g_{\Xi}, \quad \sigma(\Omega_{\chi}) \simeq \Omega_{\chi} \sigma(\hat{\Xi}^{(\text{eq})}). \end{aligned}$$

(Use this  $x$ -basis again in S5 to avoid double counting.)

**S0.8 Ward-flatness prereg thresholds** Define  $F(Q) = d\hat{\Xi}/d \ln Q$  and the normalized monitor  $F_{\sigma}(Q) = F(Q)/\sigma_{\chi}$  with masks around thresholds. The preregistered bounds are on  $F_{\sigma}$ :

$$\begin{aligned} \text{EW [80, 160] GeV} : \|F_{\sigma}\|_{\infty} &\leq 0.01430, \text{ RMS}(F_{\sigma}) \leq 0.01372, |\langle F_{\sigma} \rangle| \leq 0.01372, \\ \text{Low-GeV [1, 10] GeV} : \|F_{\sigma}\|_{\infty} &\leq 0.03535, \text{ RMS}(F_{\sigma}) \leq 0.02622, |\langle F_{\sigma} \rangle| \leq 0.02585. \end{aligned}$$

*Notes:* Bounds are preregistered from the max across 1L/off and 2L/off runs with a  $1.5\times$  inflation and include masked thresholds.

**S0.9 Versioning and pin lock** All pins in Tables 2–3 are frozen to the cited PDG/CODATA releases and mirrored locally. Section S9 provides `pins.json` (SI,  $\mu = M_Z$ ,  $\overline{\text{MS}}$ ) and scripts to regenerate Tables S0.1–S0.3 from source pins.

**Provenance** Build is deterministic: fixed RNG seeds, emitted SHA-256 hashes for each regenerated table/figure, and a manifest recording git commit and tool versions. Any drift flags a pin/version change.

## S1. Smith–Normal–Form (SNF) certificate for $\chi = (16, 13, 2)$

**Goal** Show that  $\chi$  is fixed by integer structure alone (unique primitive generator up to sign), independent of masses, scales, or scheme choices within the admissible class.

**Standing assumptions** SM with three families and one Higgs doublet; GUT-normalized hypercharge ( $\alpha_1 = \frac{5}{3}\alpha_Y$ ); mass-independent scheme with Appelquist–Carazzone decoupling. Fix a single  $U(1)_Y$  integerization so that  $U(1)$  weights are integers for each light set:

$$w_1^{(\text{f})} = 12 \sum_{\text{Weyl}} Y^2, \quad w_1^{(\text{s})} = 3 \sum_{\text{scalars}} Y^2.$$

For  $H \sim (\mathbf{1}, \mathbf{2}, \frac{1}{2})$ ,  $\sum Y^2 = 2 \times (\frac{1}{2})^2 = \frac{1}{2} \Rightarrow w_1(H) = 3$ . Ordering  $(\hat{\alpha}_s, \hat{\alpha}_2, \hat{\alpha})$  is a convention and only permutes  $\chi$ .

## S1.1 Construction recipe (per multiplet)

**Per-multiplet weights and integerization.** For each light multiplet  $f$  in an admissible window  $\mathcal{W}$ ,

$$\begin{aligned} \text{Weyl: } w_3(f) &= 4 T_{SU(3)}(f) d_{\text{spect}}(f), & w_2(f) &= 4 T_{SU(2)}(f) d_{\text{spect}}(f), \\ \text{scalar: } w_3(f) &= 1 \cdot T_{SU(3)}(f) d_{\text{spect}}(f), & w_2(f) &= 1 \cdot T_{SU(2)}(f) d_{\text{spect}}(f), \end{aligned}$$

and choose a single  $U(1)_Y$  integerizer so the hypercharge column is integral:

$$w_1^{(f)} = 12 \sum_{\text{Weyl in } f} Y^2, \quad w_1^{(s)} = 3 \sum_{\text{scalars in } f} Y^2.$$

Here  $T_{SU(N)}$  is the Dynkin index ( $T(\mathbf{3}) = T(\mathbf{2}) = \frac{1}{2}$ ), and  $d_{\text{spect}}$  counts spectator multiplicities (e.g., color for  $SU(2)$  weights and weak multiplicity for  $SU(3)$  weights). GUT normalization is used for hypercharge:  $\alpha_1 = \frac{5}{3}\alpha_Y$ .

**Window vectors and differences.** Sum the weights across the light content of the window:

$$b^{(\mathcal{W})} = \begin{pmatrix} \sum_f w_3(f) \\ \sum_f w_2(f) \\ \sum_f w_1(f) \end{pmatrix} \in \mathbb{Z}^3,$$

then form the integer *difference stack* over admissible window pairs  $\{(\mathcal{W}_i, \mathcal{W}_j)\}$ :

$$\Delta b^{(ij)} = b^{(\mathcal{W}_i)} - b^{(\mathcal{W}_j)}, \quad \Delta W = \begin{bmatrix} (\Delta b^{(i_1 j_1)})^\top \\ (\Delta b^{(i_2 j_2)})^\top \\ \vdots \end{bmatrix} \in \mathbb{Z}^{m \times 3}.$$

Adjoint self-contributions cancel in  $\Delta b$ , exposing the rank-2 lattice used for SNF.

**Sanity check (electromagnetic basis).** After EWSB, use  $w_{\text{EM}} = w_2 + \frac{5}{3}w_1 \Rightarrow 3w_{\text{EM}} = 3w_2 + 5w_1 \in \mathbb{Z}$ , so the  $(SU(3), SU(2), \text{EM})$  basis keeps exact integers for certification.

## S1.2 Worked integer kernel (by hand, no SNF)

$$\chi_{\text{EM}} = (-10, -18, 1), \quad \gcd(10, 18, 1) = 1 \text{ (primitive).}$$

In the  $(SU(3), SU(2), \text{EM})$  basis the two-row difference stack is

$$\Delta W_{\text{EM}} = \begin{bmatrix} 8 & 8 & 224 \\ 0 & 1 & 18 \end{bmatrix} \in \mathbb{Z}^{2 \times 3}.$$

Solve  $\Delta W_{\text{EM}} \chi_{\text{EM}} = 0$  over  $\mathbb{Z}$ : second row gives  $\chi_2 = -18\chi_3$ ; first row gives  $8\chi_1 + 8\chi_2 + 224\chi_3 = 0 \Rightarrow 8\chi_1 + 8(-18)\chi_3 + 224\chi_3 = 0 \Rightarrow \chi_1 = -10\chi_3$ . Choosing  $\chi_3 = 1$  yields the *primitive* generator

$$\boxed{\chi_{\text{EM}} = (-10, -18, 1), \quad \gcd(10, 18, 1) = 1.}$$

Transport to  $(\hat{\alpha}_s, \hat{\alpha}_2, \hat{\alpha})$  by the unimodular  $M$  of Sec. S1 gives

$$M^\top \chi_{\text{EM}} = (16, 13, 2) \equiv \chi.$$

*SNF note.* The Smith invariants of  $\Delta W_{\text{EM}}$  are [1, 8] (rank 2), with a trailing zero column; hence  $\ker_{\mathbb{Z}}(\Delta W_{\text{EM}})$  is one-dimensional and generated by  $\pm \chi_{\text{EM}}$ .

**SNF (explicit).** For  $\Delta W_{\text{EM}} = \begin{bmatrix} 1 & 1 & 28 \\ 0 & 1 & 18 \end{bmatrix}$ , the Smith normal form exists with unimodular  $U \in GL(2, \mathbb{Z})$ ,  $V \in GL(3, \mathbb{Z})$  such that

$$U \Delta W_{\text{EM}} V = \text{diag}(1, 8, 0),$$

so rank = 2 and there is a single zero invariant.

### S1.3 Window differences and the integer row lattice

For a momentum window  $\mathcal{W}$  with light content  $\mathcal{S}_{\mathcal{W}}$ , define integerized 1L weights

$$b^{(\mathcal{W})} = \begin{pmatrix} \sum w_3 \\ \sum w_2 \\ \sum w_1 \end{pmatrix} \in \mathbb{Z}^3,$$

with Weyl  $w_{3,2} = 4 T_{SU(3,2)} d_{\text{spect}}$  and scalar  $w_{3,2} = 1 \cdot T_{SU(3,2)} d_{\text{spect}}$ , and  $w_1$  as above. For admissible windows  $\{\mathcal{W}_i\}$  form differences

$$\Delta b^{(ij)} = b^{(\mathcal{W}_i)} - b^{(\mathcal{W}_j)}, \quad \Delta W = \begin{bmatrix} (\Delta b^{(i_1 j_1)})^\top \\ (\Delta b^{(i_2 j_2)})^\top \\ \vdots \end{bmatrix} \in \mathbb{Z}^{m \times 3}.$$

*Lemma (row-lattice invariance).* Any two admissible stacks  $\Delta W, \Delta W'$  are related by unimodular row operations (adding/removing differences; reordering) and appending/canceling common adjoint self-terms. Hence their integer row lattices coincide and their left kernels over  $\mathbb{Z}$  are identical.

$$M = \begin{bmatrix} -5 & -3 & -2 \\ 2 & 1 & 1 \\ 2 & 1 & 0 \end{bmatrix}, \quad \det M = -1, \quad M^\top \chi_{\text{EM}} = (16, 13, 2).$$

*Proof sketch.* Differences generate the same subgroup as absolute rows modulo a common reference. Appending/removing a difference corresponds to adding/removing an integer row; permutations and sign flips are unimodular. Common adjoint self-terms cancel in any row difference.  $\square$

### S1.4 Two physical differences (explicit tallies)

Using  $T(\mathbf{3}) = T(\mathbf{2}) = \frac{1}{2}$  and spectator multiplicities (weak multiplicity as spectator for  $SU(3)$  weights; color multiplicity as spectator for  $SU(2)$  weights), the integerized one-loop weights sum as follows.

**One SM generation (five Weyl multiplets).**

$$\begin{aligned} SU(3): \quad w_3(Q_L) &= 4 \cdot \frac{1}{2} \cdot 2 = 4, \quad w_3(u_R) = 4 \cdot \frac{1}{2} \cdot 1 = 2, \quad w_3(d_R) = 4 \cdot \frac{1}{2} \cdot 1 = 2 \\ \Rightarrow \sum w_3 &= 8, \end{aligned}$$

$$SU(2): \quad w_2(Q_L) = 4 \cdot \frac{1}{2} \cdot 3 = 6, \quad w_2(L_L) = 4 \cdot \frac{1}{2} \cdot 1 = 2 \Rightarrow \sum w_2 = 8,$$

$$U(1)_Y \text{ (global integerizer): } w_1 = 12 \sum_{\text{Weyl}} Y^2 = 12 \left[ \frac{1}{6} + \frac{4}{3} + \frac{1}{3} + \frac{1}{2} + 1 \right] = 40.$$

Thus

$$\Delta b_{\text{gen}} = (8, 8, 40).$$

**One Higgs doublet (complex scalar).** With  $Y = +1/2$  and two weak components,

$$w_2(H) = 1 \cdot \frac{1}{2} \cdot 1 = 1, \quad w_1(H) = 3 \sum_{\text{scalars}} Y^2 = 3 \cdot \frac{1}{2} = 3, \quad w_3(H) = 0,$$

so

$$\Delta b_H = (0, 1, 3).$$

(Any overall common integer factor on a *row* does not affect the *primitive* kernel.)

## S2. Alignment as a Symmetry-Locking Principle

**Statement.** Let  $\mathbf{K}_{\text{eq}} \succ 0$  be the equilibrium field-space metric and  $\chi = (16, 13, 2)$  the SNF-certified projector. Define  $\hat{\chi} = \chi / \|\chi\|_{\mathbf{K}_{\text{eq}}}$  and let  $e_{\text{soft}}$  be the normalized soft eigenvector of  $\mathbf{K}_{\text{eq}}$ . The *alignment condition* is

$$\cos \theta = \hat{\chi}^\top \mathbf{K}_{\text{eq}} e_{\text{soft}} \geq 1 - \varepsilon_{\text{align}},$$

with fixed tolerance  $\varepsilon_{\text{align}} \ll 1$  (reported in SM). When alignment holds, the gauge–log depth  $\hat{\Xi} = \chi \cdot \hat{\Psi}$  isolates the soft direction and the parity-even gate  $\Pi(\hat{\Xi})$  projects the gauge sector onto a single scalar depth.

**Consequences.** (i) *Even-parity protection.* A spurion  $\mathbb{Z}_2$  symmetry  $\hat{\Xi} \rightarrow -\hat{\Xi}$  with  $\Pi$  invariant implies

$$\partial_{\Xi} \Pi(\hat{\Xi}) \Big|_{\hat{\Xi}(\text{eq})} = 0 \quad \Rightarrow \quad \text{no linear response; } m_{\text{PF}}^2 = 0,$$

to all loop orders near equilibrium. Renormalization can shift  $(\sigma_\chi, \mathbf{K}_{\text{eq}})$  but cannot generate an odd term.

(ii) *Tensor sector.* Around the lab point (Minkowski) the Lichnerowicz operator reduces to

$$\Delta_L h_{\mu\nu} = -\square h_{\mu\nu} = 0 \quad \Rightarrow \quad \omega^2 = \mathbf{k}^2, \quad \lambda = \pm 2 \text{ (massless, luminal).}$$

(iii) *Quadratic lab-null.* The near-eq. response is

$$\frac{\Delta G}{G} \simeq \frac{\Delta \hat{\Xi}^2}{\sigma_\chi^2} = \frac{\varphi_\chi^2}{\Lambda_{\text{gate}}^2}, \quad \varphi_\chi = \Delta \hat{\Xi} / \|\chi\|_{\mathbf{K}_{\text{eq}}}, \quad \Lambda_{\text{gate}} = \sigma_\chi / \|\chi\|_{\mathbf{K}_{\text{eq}}}.$$

**Falsifier from misalignment.** If  $\cos \theta < 1 - \varepsilon_{\text{align}}$ , an odd (linear) term is generically induced in a lab fit

$$\frac{\Delta G}{G}(s) = A s + B s^2 + \dots,$$

violating the parity null ( $A = 0$ ). Significant misalignment therefore falsifies the model.

**Motivation (minimal).** Alignment is the universal tendency of coupled fields to cohere along the softest kinetic mode of a positive-definite metric  $K$ . In GAGE, the certified integer projector  $\chi$  aligns with the soft eigenvector of  $\mathbf{K}_{\text{eq}}$ , enforcing even response and a massless, luminal tensor sector. Analogous locking appears in magnetic ordering, superconductivity, and Higgs vacuum alignment (qualitative context; not inputs).

**S2.1 Minimal alignment functional.** Let unit order parameters  $u_i(x) \in \mathbb{R}^d$  with metrics  $K_i \succ 0$  and couplings  $\gamma_1, \gamma_2$ . Define

$$\mathcal{A}[u] = \int d^D x \left[ \frac{1}{2} \sum_i (\partial u_i)^\top K_i (\partial u_i) - \frac{1}{N} \sum_{i < j} (\gamma_1 u_i \cdot u_j + \gamma_2 (u_i \cdot u_j)^2) \right], \quad \|u_i\| = 1.$$

Diagnostics  $m = \|\langle u \rangle\|$ ,  $C = \frac{1}{N} \sum_i u_i u_i^\top$ , and  $\rho = \lambda_{\max}(C)/\text{Tr}(C)$  measure coherence ( $m \in [0, 1]$ ,  $\rho \in [1/d, 1]$ ).

**Lemma.** For  $K \succ 0$  and couplings above a threshold  $\gamma_c$ , minimizers align  $\langle u \rangle$  with the soft eigenvector  $e_{\text{soft}}$  of  $K$  up to  $O(\kappa_{\text{gap}}^{-1})$ ; orthogonal fluctuations are gapped. **Map to GAGE.**  $u \parallel \hat{\chi}$ ,  $K \rightarrow \mathbf{K}_{\text{eq}}$ ,  $\Xi = \chi \cdot \hat{\Psi}$ , and even  $\Pi(\Xi)$  enforces  $\frac{\Delta G}{G} \simeq \varphi_\chi^2 / \Lambda_{\text{gate}}^2$ .

**S2.2 Phase variant (S<sup>1</sup>).** For phases  $\theta_i$ ,

$$\mathcal{A}_\theta[\theta] = \int d^Dx \left[ \frac{\kappa}{2} \sum_i |\nabla \theta_i|^2 - \frac{K}{N} \sum_{i < j} \cos(\theta_i - \theta_j) \right],$$

whose ordered phase satisfies  $\partial_\mu \theta_i \approx \partial_\mu \theta_j$ , corresponding to alignment of phase gradients.

**S2.3 Conservation form (near equilibrium).** Define the alignment current

$$J_{\text{align}}^\mu = \Pi(\Xi) \chi^\top \mathbf{K}_{\text{eq}} \partial^\mu \hat{\Psi},$$

which reduces after one contraction to  $J_{\text{align}}^\mu = \Pi(\Xi) \partial^\mu \Xi$ . Using  $\Pi'(\Xi_{\text{eq}}) = 0$  and the  $\Xi$  equation of motion,

$$\partial_\mu J_{\text{align}}^\mu = 0 + \mathcal{O}((\Delta \hat{\Xi})^3, \text{two-loop drift, } \varepsilon_{\text{align}}).$$

Any measured odd term  $A \neq 0$  in  $\frac{\Delta G}{G} = A s + B s^2 + \dots$  gives  $\partial_\mu J_{\text{align}}^\mu \neq 0$  and falsifies alignment.

**S2.4 Information-geometry view.** The Fisher curvature  $\kappa_\chi = 1/\sigma_\chi^2$  defines the local informational metric. Alignment is motion along the soft eigenvector of  $\mathbf{K}_{\text{eq}}$ , the direction of least informational curvature.

**S2.5 Falsifiers and caveats.** Falsifiers include a persistent odd response ( $A \neq 0$ ), failure of rank-1 coherence ( $\rho \not\rightarrow 1$ ), or alignment to a non-soft mode at fixed  $K$ . Boundary or disorder effects can produce modulated/defect states; diagnose via the most unstable Fourier mode of the quadratic expansion.

**S2.6 Cross-domain statement.** Across spins, phases, and gauge directions, alignment is symmetry locking to the soft mode of  $K$ , quantified by  $(m, \rho)$ . GAGE is the SM realization with  $u \parallel \hat{\chi}$  and  $K = \mathbf{K}_{\text{eq}}$ .

## S3. Gate, parity lemma, and quadratic response

### S3.1 Even gate $\Pi(\Xi)$ and normalization

Promote  $\hat{\Xi} = \chi \cdot \hat{\Psi}$  to a spacetime scalar  $\hat{\Xi}(x)$  via  $\hat{\Psi}(x)$ . Define a parity-even projection gate

$$\frac{G \Pi(\hat{\Xi})}{G} = \Pi(\hat{\Xi}), \quad \Pi((\hat{\Xi}^{(\text{eq})})) = 1, \quad \Pi((\hat{\Xi}^{(\text{eq})} + \Delta)) = \Pi((\hat{\Xi}^{(\text{eq})} - \Delta)),$$

with  $\Pi$  assumed  $C^2$  near  $\hat{\Xi}^{(\text{eq})}$  and depending only on  $\hat{\Xi}$ . It introduces no gravitational dynamics beyond a multiplicative normalization.

**Gaussian model (optional, for figures/tests)** For numerical plots we sometimes use the Gaussian ansatz

$$\Pi_G(\Xi) = \exp \left[ -\frac{(\Xi - \hat{\Xi}^{(\text{eq})})^2}{\sigma_\chi^2} \right],$$

but all derivations require only evenness and smoothness.

### S3.2 Parity lemma and quadratic response

Let  $\Delta \hat{\Xi} \equiv \hat{\Xi} - \hat{\Xi}^{(\text{eq})}$ . Evenness implies  $\partial_\Xi \Pi()|_{\hat{\Xi}^{(\text{eq})}} = 0$  and

$$\Pi((\hat{\Xi}^{(\text{eq})} + \Delta \hat{\Xi})) = 1 + \frac{1}{2} \Pi('(\hat{\Xi}^{(\text{eq})}) \Delta \hat{\Xi}^2 + \mathcal{O}((\Delta \hat{\Xi})^3)).$$

Hence

$$\frac{\Delta G}{G} = \frac{G \Pi(\hat{\Xi})}{G} - 1 = \Pi((\hat{\Xi}^{(\text{eq})} + \Delta \hat{\Xi})) - 1 \simeq \frac{1}{2} \Pi('(\hat{\Xi}^{(\text{eq})}) \Delta \hat{\Xi}^2),$$

and all odd corrections vanish:  $\partial_\Xi^{(2k+1)} \Pi()|_{\hat{\Xi}^{(\text{eq})}} = 0$ . For  $\Pi_G$ ,  $\Pi_G''(\hat{\Xi}^{(\text{eq})}) = -2/\sigma_\chi^2$ , so  $|\Delta G/G| \simeq \Delta \hat{\Xi}^2 / \sigma_\chi^2$ .

### S3.3 Soft mode, canonical form, and $\Lambda_{\text{gate}} = \sigma_\chi / \|\chi\|_{\mathbf{K}_{\text{eq}}}$

With  $\mathbf{K}_{\text{eq}} \succ 0$  (Table 5), define

$$\varphi_\chi = \frac{\chi^\top (\hat{\Psi} - \hat{\Psi}_{\text{eq}})}{\|\chi\|_{\mathbf{K}_{\text{eq}}}}, \quad \|\chi\|_{\mathbf{K}_{\text{eq}}} = \sqrt{\chi^\top \mathbf{K}_{\text{eq}} \chi},$$

so  $\Delta \hat{\Xi} = \|\chi\|_{\mathbf{K}_{\text{eq}}} \varphi_\chi$ . A convenient canonical parameterization is

$$\Pi(\hat{\Xi}) = \exp\left[-\frac{\varphi_\chi^2}{\Lambda_{\text{gate}}^2}\right], \quad \Lambda_{\text{gate}} = \frac{\sigma_\chi}{\|\chi\|_{\mathbf{K}_{\text{eq}}}},$$

and near equilibrium  $|\Delta G/G| \simeq \varphi_\chi^2/\Lambda_{\text{gate}}^2$ . The macros encode

$$\omega_{\text{hel}} = \frac{\|\chi\|_{\mathbf{K}_{\text{eq}}}}{\sigma_\chi} = \frac{1}{\Lambda_{\text{gate}}}, \quad T_{\text{hel}} = \frac{2\pi}{\omega_{\text{hel}}} = 2\pi \Lambda_{\text{gate}}.$$

### S3.4 Spurion $\mathbb{Z}_2$ and radiative stability (all orders)

**Definition (spurion parity).** Assign the *spurionic* reflection symmetry in gauge-log space

$$\Xi \mapsto -\Xi, \quad \delta\Xi \mapsto -\delta\Xi, \quad \Pi \mapsto \Pi,$$

and act trivially on directions orthogonal to  $\chi$ :  $P_\perp(\hat{\Psi} - \hat{\Psi}_{\text{eq}}) \mapsto P_\perp(\hat{\Psi} - \hat{\Psi}_{\text{eq}})$  with  $P_\perp = \mathbb{1} - P_\chi$  and  $P_\chi = \mathbf{K}_{\text{eq}} \chi \chi^\top / (\chi^\top \mathbf{K}_{\text{eq}} \chi)$ .

**Lemma (operator classification near  $\hat{\Xi}^{(\text{eq})}$ ).** In a local EFT respecting the spurion parity and the residual  $O(2)$  rotations in the orthogonal complement, any scalar functional that multiplies the Ricci term must be built from *even* invariants:

$$\Pi(\Xi, \partial\Xi, \dots) = \Pi_0 + \Pi_2 \frac{\delta\Xi^2}{\sigma_\chi^2} + \Pi_{2,\partial} \frac{(\partial\delta\Xi)^2}{\Lambda_{\text{gate}}^2} + \dots,$$

while all terms linear in  $\delta\Xi$  or odd in derivatives are forbidden.

**Radiative stability (renormalization statement).** Loop corrections consistent with the spurion parity cannot generate a linear term:  $\partial_\Xi \Pi|_{\hat{\Xi}^{(\text{eq})}}$  renormalizes multiplicatively to zero. Allowed counterterms renormalize (i) the overall normalization  $\Pi(\hat{\Xi}^{(\text{eq})}) \equiv 1$  (fixed by calibration), (ii) the width  $\sigma_\chi$ , (iii) the kinetic metric  $K_{ij}$ , and higher-even coefficients. Hence the *only* effect at quadratic order is a finite renormalization of  $\sigma_\chi$  and  $K_{ij}$ ; no  $\mathcal{O}((\Delta \hat{\Xi})^2)$  response appears to any loop order.

### S3.5 Why $\Pi = \Pi(\Xi)$ (no dependence on orthogonal modes)

By construction  $\Xi = \chi \cdot \hat{\Psi}$  is the unique (primitive) integer depth (S1). Near equilibrium, the orthogonal subspace is two-dimensional; imposing the residual  $O(2)$  symmetry in  $P_\perp$  forbids any dependence on a specific orthogonal direction at leading order. Therefore the most general scalar gate consistent with these symmetries is a function of  $\Xi$  alone (plus *even* derivative corrections as in S3.4), which are higher order in the lab-null setups of S6.

### S3.6 Falsifier (boxed, S6 handoff)

$$\partial_\Xi \Pi(\Xi)|_{\hat{\Xi}^{(\text{eq})}} = 0 \implies \text{no linear term in } \frac{\Delta G}{G}. \text{ Any observed } \mathcal{O}(\Delta \hat{\Xi}) \text{ signal falsifies the construction.}$$

The quadratic coefficient is  $\frac{1}{2} \Pi''(\hat{\Xi}^{(\text{eq})})$  (Gaussian:  $-2/\sigma_\chi^2$ ). The lab-null template and two-state contrast appear in S6.

**Parity reminder.** At  $\hat{\Psi}_{\text{eq}}$ ,  $\partial_{\Xi}\Pi|_{\text{eq}} = 0$ ; hence no linear (odd) term in  $\delta\Xi$  appears and leading deviations are  $\propto \delta\Xi^2$ .

## S4. Tensor sector and absence of Pauli–Fierz mass

### S4.1 Background, Jordan-frame expansion, and kinetic structure

Assume a stationary, flat laboratory background

$$\hat{\Psi} = \hat{\Psi}_{\text{eq}}, \quad \partial_{\hat{\Psi}} V|_{\hat{\Psi}_{\text{eq}}} = 0, \quad V(\hat{\Psi}_{\text{eq}}) = 0, \quad g_{\mu\nu} = \eta_{\mu\nu} + h_{\mu\nu}.$$

Insert the gate into the Einstein–Hilbert term:

$$S = \int d^4x \sqrt{-g} \left[ \frac{1}{2} M_P^2 \Pi(\hat{\Xi}) R - \frac{1}{2} \partial_{\mu} \hat{\Psi}^{\top} \mathbf{K}(\hat{\Psi}) \partial^{\mu} \hat{\Psi} - V(\hat{\Psi}) \right].$$

At equilibrium  $\Pi(\hat{\Xi}^{(\text{eq})}) = 1$  and, by S2,  $\partial_{\Xi}\Pi(\Xi)|_{\hat{\Xi}^{(\text{eq})}} = 0$ . Expand around  $g_{\mu\nu} = \eta_{\mu\nu} + h_{\mu\nu}$  in harmonic gauge  $\partial^{\mu}h_{\mu\nu} - \frac{1}{2}\partial_{\nu}h = 0$ . To quadratic order in  $h$ ,

$$S_{\text{tens}}^{(2)} = \frac{M_P^2}{8} \int d^4x h^{\mu\nu} \mathcal{E}_{\mu\nu}^{\alpha\beta} h_{\alpha\beta} + \mathcal{O}(h^2 \Delta \hat{\Xi}^2),$$

where  $\mathcal{E}$  is the Lichnerowicz operator. Since  $\Pi'(\hat{\Xi}^{(\text{eq})}) = 0$ , all potential  $h^2 \Delta \hat{\Xi}$  mixings vanish.

**No Pauli–Fierz mass.** Around flat equilibrium with  $\Pi'(\hat{\Xi}^{(\text{eq})}) = 0$  and  $\Pi(\hat{\Xi}^{(\text{eq})}) = 1$ , the linearized tensor sector equals GR’s: no  $m_{\text{PF}}^2(h_{\mu\nu}h^{\mu\nu} - h^2)$  term appears. Gate effects begin at  $\mathcal{O}((\Delta \hat{\Xi}^2))$  and do not alter the kinetic Lichnerowicz form.

**Kinetic metric and soft-mode projectors** The log-coupling fields expand with

$$\mathcal{L}_{\text{kin}} = -\frac{1}{2} \partial_{\mu} \hat{\Psi}^{\top} \mathbf{K}(\hat{\Psi}) \partial^{\mu} \hat{\Psi}, \quad \mathbf{K}_{\text{eq}} = \mathbf{K}(\hat{\Psi})|_{\hat{\Psi}_{\text{eq}}} \succ 0.$$

Define the  $\mathbf{K}_{\text{eq}}$ -unit vector and projectors

$$\hat{u}_{\chi} = \frac{\chi}{\|\chi\|_{\mathbf{K}_{\text{eq}}}}, \quad P_{\chi} = \hat{u}_{\chi} \hat{u}_{\chi}^{\top} \mathbf{K}_{\text{eq}}, \quad P_{\perp} = \mathbb{1} - P_{\chi},$$

so  $\varphi_{\chi} = \hat{u}_{\chi}^{\top} \mathbf{K}_{\text{eq}} (\hat{\Psi} - \hat{\Psi}_{\text{eq}})$ , and  $\Delta \hat{\Xi} = \chi \cdot (\hat{\Psi} - \hat{\Psi}_{\text{eq}}) = \|\chi\|_{\mathbf{K}_{\text{eq}}} \varphi_{\chi}$ . The explicit  $\mathbf{K}_{\text{eq}}$  and eigenstructure appear in Tables 5–6.

### S4.2 Explicit origin of the no-mixing result

Vary the Jordan-frame Ricci term with  $\Omega(\hat{\Psi}) \equiv M_P^2 \Pi(\Xi)$ :

$$\delta(\sqrt{-g} \Omega R) = \sqrt{-g} \left[ \frac{1}{2} \Omega h^{\mu\nu} \mathcal{E}_{\mu\nu}^{\alpha\beta} h_{\alpha\beta} + (g_{\mu\nu} \square - \nabla_{\mu} \nabla_{\nu}) \delta\Omega h^{\mu\nu} \right]_{\text{lin}} + \dots$$

Near equilibrium,  $\delta\Omega = M_P^2 \Pi'(\hat{\Xi}^{(\text{eq})}) \delta\Xi + \mathcal{O}((\delta\Xi^2)) = 0 + \mathcal{O}((\delta\Xi^2))$ , so the would-be  $h \delta\Xi$  mixing proportional to  $(\partial\partial \delta\Omega)$  is absent at linear order. The first nonzero gate correction is  $\mathcal{O}(h \delta\Xi^2)$ , which cannot produce a Pauli–Fierz mass term and instead renormalizes higher-order interactions.

### S4.3 GR limit and field equations (linearized)

Collect the  $\mathcal{O}((h))$  terms and couple to conserved matter  $T_{\mu\nu}$ :

$$M_P^2 \mathcal{E}_{\mu\nu}^{\alpha\beta} h_{\alpha\beta} = T_{\mu\nu} + \mathcal{O}(h \delta \Xi^2).$$

The gauge symmetries and propagator match GR; the two tensor polarizations propagate luminally with  $k^2 = 0$ . The Newtonian potentials satisfy

$$\nabla^2 \Phi = \nabla^2 \Psi = \frac{1}{2} M_P^{-2} T_{00} \Rightarrow \gamma \equiv \Psi/\Phi = 1 + \mathcal{O}(\Delta \hat{\Xi}^2 / \sigma_\chi^2),$$

consistent with the parity lemma (S2): odd response is forbidden and leading deviations are quadratic.

### S4.4 Even scalar sector and width provenance

To parameterize widths without inducing a PF mass, use a parity-even quadratic potential in field space:

$$V(\hat{\Psi}) = \frac{1}{2} (\hat{\Psi} - \hat{\Psi}_{\text{eq}})^\top \Sigma_\perp^{-1} P_\perp (\hat{\Psi} - \hat{\Psi}_{\text{eq}}) + \frac{\gamma}{2} (\chi \cdot (\hat{\Psi} - \hat{\Psi}_{\text{eq}}))^2,$$

with  $\Sigma_\perp^{-1} \succ 0$  on  $P_\perp$  and  $\gamma > 0$ . The Hessian at equilibrium is

$$H \equiv \partial_i \partial_j V|_{\text{eq}} = \Sigma_\perp^{-1} P_\perp + \gamma \chi \chi^\top.$$

The canonically normalized soft-mode mass is

$$m_\chi^2 = \frac{\chi^\top H \chi}{\chi^\top \mathbf{K}_{\text{eq}} \chi} = \frac{\chi^\top \Sigma_\perp^{-1} P_\perp \chi}{\chi^\top \mathbf{K}_{\text{eq}} \chi} + \gamma \frac{(\chi^\top \chi)^2}{\chi^\top \mathbf{K}_{\text{eq}} \chi}.$$

Since  $P_\perp \chi = 0$ ,

$$m_\chi^2 = \gamma \frac{(\chi^\top \chi)^2}{\chi^\top \mathbf{K}_{\text{eq}} \chi} \equiv \gamma_\chi \|\chi\|_{\mathbf{K}_{\text{eq}}}^{-2}, \quad \gamma_\chi \equiv \gamma (\chi^\top \chi)^2.$$

An even scalar potential thus produces widths in the scalar sector while preserving the massless, luminal spin-2 sector and forbidding any linear  $h$ - $\delta \Xi$  mixing.

### S4.5 Covariant embedding (summary and cross-ref)

With

$$S = \int \sqrt{-g} \left[ \frac{1}{2} \Omega(\hat{\Psi}) R - \frac{1}{2} G_{ij}(\hat{\Psi}) \nabla_\mu \xi^i \nabla^\mu \xi^j - V(\hat{\Psi}) + L_{\text{gauge}} + L_{\text{matter}} \right],$$

metric variation yields

$$\Omega G_{\mu\nu} + (g_{\mu\nu} \square - \nabla_\mu \nabla_\nu) \Omega = T_{\mu\nu}^{(\Psi)} + T_{\mu\nu}^{\text{gauge}} + T_{\mu\nu}^{\text{matter}}.$$

Calibrating  $\Omega(\hat{\Psi}_{\text{eq}}) = M_P^2$  (i.e.,  $\Pi(\hat{\Xi}^{(\text{eq})}) = 1$ ) and using  $\Pi'(\hat{\Xi}^{(\text{eq})}) = 0$  gives the GR quadratic sector exactly; expanding in  $\delta \Xi$  reproduces the quadratic response of S3 with leading deviation  $\Delta G/G \simeq \Delta \hat{\Xi}^2 / \sigma_\chi^2$ .

### S4.6 Equilibrium metric and spectrum

**Kinetic term (equilibrium metric)** Work in log-coupling coordinates

$$\hat{\Psi} = (\ln \hat{\alpha}_s, \ln \hat{\alpha}_2, \ln \hat{\alpha}) = (\ln \hat{\alpha}_s, \ln \hat{\alpha}_2, \ln \hat{\alpha}), \quad \hat{\Xi} = \chi \cdot \hat{\Psi}, \quad \chi = (16, 13, 2).$$

The scalar kinetic Lagrangian is

$$\mathcal{L}_{\text{kin}} = -\frac{1}{2} \partial_\mu \hat{\Psi}^\top \mathbf{K}(\hat{\Psi})(\hat{\Psi}) \partial^\mu \hat{\Psi}, \quad \mathbf{K}(\hat{\Psi})(\hat{\Psi}) \succ 0 \quad (1)$$

and at the equilibrium point

$$\mathbf{K}_{\text{eq}} \equiv \mathbf{K}(\hat{\Psi})(\hat{\Psi}_{\text{eq}}) = \begin{bmatrix} 1.2509 & -0.6202 & -0.1813 \\ -0.6202 & 1.5128 & -0.1633 \\ -0.1813 & -0.1633 & 3.2362 \end{bmatrix}, \quad \mathbf{K}_{\text{eq}} \succ 0. \quad (2)$$

**Spectrum and alignment** Let  $\{\lambda_i, e_i\}$  be the orthonormal eigenpairs of  $\mathbf{K}_{\text{eq}}$  (Euclidean inner product):

$$\lambda_{\min} = 0.7243366, \quad \lambda_2 = 2.0155976, \quad \lambda_{\max} = 3.2599658,$$

with

$$e_{\text{soft}} = (0.7724942, 0.6276375, 0.0965604), \quad \mathbf{K}_{\text{eq}} = \sum_{i=1}^3 \lambda_i e_i e_i^\top.$$

Numerically,

$$\hat{\chi} \equiv \frac{\chi}{\|\chi\|_2} = (0.7724873, 0.6276459, 0.0965609), \quad \cos \theta_{\mathbf{K}_{\text{eq}}} := \hat{\chi} \cdot e_{\text{soft}} = 1.0000000 \pm \mathcal{O}(10^{-8}),$$

and

$$\mathbf{K}_{\text{eq}} \chi = \lambda_{\min} \chi \pm \mathcal{O}(10^{-4}) \quad (\text{componentwise}).$$

Thus  $\chi$  aligns with the soft eigenmode within numerical precision.

### Metric-aware projectors (canonical)

$$P_\chi = \frac{\chi \chi^\top \mathbf{K}_{\text{eq}}}{\chi^\top \mathbf{K}_{\text{eq}} \chi}, \quad P_\perp = \mathbb{1} - P_\chi$$

(3)

### Consequences (used throughout)

- **Depth norm:**  $\|\chi\|_{\mathbf{K}_{\text{eq}}}^2 = \chi^\top \mathbf{K}_{\text{eq}} \chi = \lambda_{\min} \chi^\top \chi = \lambda_{\min} \times 429 \Rightarrow \|\chi\|_{\mathbf{K}_{\text{eq}}} = 17.6278$ .
- **Gate scale:** with even curvature–gate width  $\sigma_\chi = 247.683$ ,  $\Lambda_{\text{gate}} = \sigma_\chi / \|\chi\|_{\mathbf{K}_{\text{eq}}} = 14.052$ ,  $\omega_{\text{hel}} = \Lambda_{\text{gate}}^{-1} = 0.0712$ ,  $T_{\text{hel}} = 2\pi \Lambda_{\text{gate}} \simeq 88 t_P$ .
- **Softest direction:** for any displacement  $\omega$ , the quadratic form  $Q(\omega) = \omega^\top \mathbf{K}_{\text{eq}} \omega$  is minimized along the  $\chi$  direction; orthogonal motion costs more.

**Eigen-decomposition and positivity** Let  $R = [e_1 \ e_2 \ e_3]$  be orthogonal. Then

$$R^\top \mathbf{K}_{\text{eq}} R = \text{diag}(\lambda_1, \lambda_2, \lambda_3), \quad \lambda_i > 0. \quad (4)$$

**Depth direction and  $\mathbf{K}_{\text{eq}}$  norm** For  $\chi = (16, 13, 2)$ , define

$$\|\chi\|_{\mathbf{K}_{\text{eq}}}^2 := \chi^\top \mathbf{K}_{\text{eq}} \chi, \quad \hat{\chi}_{\mathbf{K}_{\text{eq}}} := \frac{\chi}{\sqrt{\chi^\top \mathbf{K}_{\text{eq}} \chi}}, \quad \hat{\chi} := \frac{\chi}{\|\chi\|_2}. \quad (5)$$

(The alternative  $\mathbf{K}_{\text{eq}} \chi \chi^\top / (\chi^\top \mathbf{K}_{\text{eq}} \chi)$  sometimes seen in the literature is *not* the  $\mathbf{K}_{\text{eq}}$ –orthogonal projector on column vectors.)

### S4.7 Scalar potential, widths, and consistency certificate

**Purpose** The scalar potential below is not required for graviton emergence or GR normalization (those follow from the parity of the curvature gate  $\Pi(\Xi)$ ; see S2/S3.2). This section only certifies that one can assign a consistent EFT width to the depth mode and regulate transverse directions without inducing a Pauli–Fierz mass or linear mixing.

**Scalar potential (parity-even, quadratic)** In log-coupling space write

$$\hat{\Psi} = (\ln \hat{\alpha}_s, \ln \hat{\alpha}_2, \ln \hat{\alpha}) = (\ln \hat{\alpha}_s, \ln \hat{\alpha}_2, \ln \hat{\alpha}), \quad \chi = (16, 13, 2), \quad \hat{\Xi} = \chi \cdot \hat{\Psi},$$

and define  $\Delta \hat{\Psi} = \hat{\Psi} - \hat{\Psi}_{\text{eq}}$ ,  $\hat{\Xi}^{(\text{eq})} = \chi \cdot \hat{\Psi}_{\text{eq}}$ . Take

$$V(\hat{\Psi}) = \frac{1}{2} \sum_{i \in \{s, 2, e\}} \frac{(\xi_i - \xi_i^{(\text{eq})})^2}{\sigma_i^2} + \frac{\gamma}{2} (\chi \cdot \Delta \hat{\Psi})^2, \quad (6)$$

so parity about  $\hat{\Xi}^{(\text{eq})}$  is manifest:  $\partial_{\xi_i} V|_{\text{eq}} = 0$  and all odd powers in  $(\chi \cdot \Delta \hat{\Psi})$  vanish.

**Equivalent projector/operator form (metric-correct)** Let

$$P_\chi = \frac{\chi \chi^\top \mathbf{K}_{\text{eq}}}{\chi^\top \mathbf{K}_{\text{eq}} \chi}, \quad P_\perp = \mathbb{1} - P_\chi, \quad \mathbf{K}_{\text{eq}} \succ 0.$$

Then an equivalent form that makes the transverse restriction explicit is

$$V(\hat{\Psi}) = \frac{1}{2} \Delta \hat{\Psi}^\top (P_\perp \Sigma_\perp^{-1} P_\perp) \Delta \hat{\Psi} + \frac{\gamma}{2} (\chi \cdot \Delta \hat{\Psi})^2, \quad \Sigma_\perp^{-1} = \text{diag}\left(\frac{1}{\sigma_{\alpha_s}^2}, \frac{1}{\sigma_{\alpha_2}^2}, \frac{1}{\sigma_\alpha^2}\right). \quad (7)$$

(Using  $P_\perp = \mathbb{1} - \mathbf{K}_{\text{eq}} \chi \chi^\top / (\chi^\top \mathbf{K}_{\text{eq}} \chi)$  would *not* be the  $\mathbf{K}_{\text{eq}}$ -orthogonal projector on column vectors; the form above is the correct one.)

**Parameter choices (depth vs transverse) Depth (derived, fixed).** From Tables 5 and 4:

$$\sigma_\chi = 247.683, \quad \|\chi\|_{\mathbf{K}_{\text{eq}}} = 17.6278, \quad \Lambda_{\text{gate}} = \frac{\sigma_\chi}{\|\chi\|_{\mathbf{K}_{\text{eq}}}} = 14.052, \quad \omega_{\text{hel}} = \Lambda_{\text{gate}}^{-1} = 0.0712, \quad T_{\text{hel}} = 2\pi \Lambda_{\text{gate}} \simeq 88 t_P.$$

These follow from the Fisher curvature (gate width) and the kinetic norm.

**Transverse (regulator pins, fixed once).** The transverse widths regulate only the  $P_\perp$  plane:

$$\sigma_{\alpha_s} = 0.446296, \quad \sigma_{\alpha_2} = 0.547533, \quad \sigma_\alpha = 0.551281.$$

They do not affect the GR tensor sector (which depends only on gate parity; see S2/S3.2).

**Isotropic fallback (metric-aware).** If a symbolic fallback is desired, impose isotropy in the  $\mathbf{K}_{\text{eq}}$ -metric subspace orthogonal to  $\chi$ :

$$\boxed{\Sigma_\perp = C P_\perp, \quad P_\perp = \mathbb{1} - \frac{\chi \chi^\top \mathbf{K}_{\text{eq}}}{\chi^\top \mathbf{K}_{\text{eq}} \chi}}$$

i.e., equal variance in any direction orthogonal to  $\chi$ . (Componentwise recipes like  $\sigma_i \propto |\chi_i|$  are not isotropic in the  $\mathbf{K}_{\text{eq}}$  metric and should be avoided.)

**Hessian and depth-mode mass** Expanding (7),

$$H \equiv \partial_i \partial_j V|_{\text{eq}} = P_\perp \Sigma_\perp^{-1} P_\perp + \gamma \chi \chi^\top. \quad (8)$$

Project along  $\chi$  and normalize by  $\mathbf{K}_{\text{eq}} \succ 0$ :

$$m_\chi^2 = \frac{\chi^\top H \chi}{\chi^\top \mathbf{K}_{\text{eq}} \chi} = \frac{\chi^\top P_\perp \Sigma_\perp^{-1} P_\perp \chi}{\chi^\top \mathbf{K}_{\text{eq}} \chi} + \gamma \frac{(\chi^\top \chi)^2}{\chi^\top \mathbf{K}_{\text{eq}} \chi}. \quad (9)$$

Since  $P_\perp \chi = 0$  by construction, the soft mass reduces to the depth-only certificate

$$\boxed{m_\chi^2 = \gamma \frac{(\chi^\top \chi)^2}{\chi^\top \mathbf{K}_{\text{eq}} \chi} = \gamma_\chi \|\chi\|_{\mathbf{K}_{\text{eq}}}^{-2}, \quad \gamma_\chi \equiv \gamma (\chi^\top \chi)^2}, \quad (10)$$

i.e. curvature resides only along the  $\chi$  direction.

**Transverse regulator implementation** With the  $\mathbf{K}_{\text{eq}}$ -metric projectors above, implement the regulator as  $P_\perp \Sigma_\perp^{-1} P_\perp$ . This leaves the depth gate and tensor sector unchanged and avoids spurious mixing.

**Gate in canonical form and parity lemma (recap)** Define

$$\varphi_\chi = \frac{\chi^\top (\hat{\Psi} - \hat{\Psi}_{\text{eq}})}{\|\chi\|_{\mathbf{K}_{\text{eq}}}}, \quad \Delta \hat{\Xi} = \|\chi\|_{\mathbf{K}_{\text{eq}}} \varphi_\chi,$$

so

$$\boxed{\Pi(\Xi) = \exp\left[-\frac{\varphi_\chi^2}{\Lambda_{\text{gate}}^2}\right], \quad \Lambda_{\text{gate}} = \frac{\sigma_\chi}{\|\chi\|_{\mathbf{K}_{\text{eq}}}}}, \quad (11)$$

and near equilibrium  $|\Delta G/G| \simeq \varphi_\chi^2 / \Lambda_{\text{gate}}^2$  with the odd (linear) term absent:  $\partial_\Xi \Pi|_{\hat{\Xi}(\text{eq})} = 0 \Rightarrow$  no  $h\varphi$  linear mixing, no Pauli–Fierz mass.

**Expansion about equilibrium and quadratic Lagrangian** Set  $\hat{\Psi} = \hat{\Psi}_{\text{eq}} + \varphi$  and  $g_{\mu\nu} = \eta_{\mu\nu} + h_{\mu\nu}$ . With  $M_*^2 := M_P^2 \Pi(\Xi)|_{\hat{\Psi}=\hat{\Psi}_{\text{eq}}} = M_P^2$  and  $\Delta\hat{\Xi} = \chi \cdot \varphi$ ,

$$\Pi(\Xi) = 1 - \Delta\hat{\Xi}^2/\sigma_\chi^2 + \mathcal{O}((\varphi)^4).$$

To quadratic order,

$$\mathcal{L}^{(2)} = \frac{M_*^2}{8} h^{\mu\nu} \mathcal{E}_{\mu\nu}^{\rho\sigma} h_{\rho\sigma} - \frac{1}{2} \partial_\mu \varphi^\top \mathbf{K}_{\text{eq}} \partial^\mu \varphi - \frac{1}{2} \varphi^\top M^2 \varphi + \mathcal{O}(h^2 \varphi^2) + \mathcal{O}(h^2 \varphi), \quad (12)$$

with  $M^2 = P_\perp \Sigma_\perp^{-1} P_\perp + \gamma \chi \chi^\top$  and  $\mathcal{E}$  the Lichnerowicz operator. By parity, linear  $h \cdot \varphi$  mixing cancels and the graviton is massless and luminal.

**Weinberg soft factor (unchanged)** In the  $q \rightarrow 0$  limit,

$$\mathcal{M}_{n+1} \simeq \kappa S^{(0)}(q, \varepsilon) \mathcal{M}_n, \quad S^{(0)} = \sum_{i=1}^n \eta_i \frac{p_i^\mu p_i^\nu \varepsilon_{\mu\nu}}{p_i \cdot q}, \quad \kappa = \frac{2}{M_*},$$

$\eta_i = \pm 1$ , and  $\varepsilon_{\mu\nu}$  is transverse and traceless. Depth parity at the lab point leaves  $S^{(0)}$  invariant.

**Light deflection** Because  $\Pi(\Xi) = 1 + \mathcal{O}((\Delta\hat{\Xi})^2)$ , the leading eikonal angle is the GR value

$$\theta = \frac{4G M}{b c^2},$$

with fractional corrections  $\mathcal{O}((\Delta\hat{\Xi}/\sigma_\chi)^2)$ ; in PPN language  $\gamma_{\text{PPN}} = 1 + \mathcal{O}((\Delta\hat{\Xi}/\sigma_\chi)^2)$ . (At equilibrium,  $G=G_N$  by calibration.)

**One-loop counterterm container map (near equilibrium)** Divergences renormalize only  $\{\Pi(\Xi), \mathbf{K}_{\text{eq}}, V(\hat{\Psi})\}$  and higher curvature. No linear  $\Delta\hat{\Xi}$  counterterm appears by parity. Finite parts are absorbed as:

**Positivity and bounds** Working near equilibrium with diagonal tensor and regulated scalar sectors, require

$$\mathbf{K}_{\text{eq}} \succ 0, \quad \sigma_\chi^2 > 0, \quad \gamma > 0, \quad M_*^2 = M_P^2 \Pi(\hat{\Xi}^{(\text{eq})}) > 0,$$

ensuring GR tensor propagation and a stable scalar sector with no linear fifth force.

## S5. RG running and Ward-flatness monitor

### S5.1 Definition and admissible windows

**Running-depth observable.** In the  $\overline{\text{MS}}$  scheme define

$$F(Q) \equiv \beta_\Xi(Q) = \chi \cdot \frac{d\hat{\Psi}}{d\ln Q} = 16 \frac{d(\ln \hat{\alpha}_s)}{d\ln Q} + 13 \frac{d(\ln \hat{\alpha}_2)}{d\ln Q} + 2 \frac{d(\ln \hat{\alpha})}{d\ln Q}, \quad (13)$$

with  $\hat{\Psi} = (\ln \hat{\alpha}_s, \ln \hat{\alpha}_2, \ln \hat{\alpha})$  and  $\chi = (16, 13, 2)$ .

**Admissible windows.** A window  $\mathcal{W}$  is admissible if the particle content is fixed (mass-independent scheme), all heavy thresholds lie outside  $\mathcal{W}$ , and the EM basis is used post-EWSB. Within any such  $\mathcal{W}$ , Appelquist–Carazzone decoupling applies and the Smith–normal–form identity

$$\chi \cdot b^{(\mathcal{W})} = 0 \quad (\text{one loop, GUT normalization}) \quad (14)$$

cancels the  $\alpha$ -independent one-loop drift. Writing

$$F^{(1\text{L})}(Q) = \frac{1}{2\pi} \sum_{i=1}^3 \chi_i b_i \alpha_i(Q), \quad (15)$$

the coupling weights  $\alpha_i(Q)$  prevent an exact zero away from the pivot, so small residuals remain; these are the target of the preregistered bands.

**Masked windows (preregistered).** We evaluate  $F$  on

$$W_{\text{EW}} = 80 \text{ GeV to } 160 \text{ GeV}, \quad W_{\text{GeV}} = 1 \text{ GeV to } 10 \text{ GeV},$$

sampling  $Q$  logarithmically and excising symmetric guard bands around thresholds prior to statistics on  $F_\sigma$ . Table 12 lists the masks used in all runs.

Masks are applied within  $W_{\text{EW}}$  and  $W_{\text{GeV}}$ . Grid and mask variations ( $\pm 20\%$  step,  $\pm 25\%$  mask half-width) leave pass/fail unchanged (Sec. S5.2).

**Rationale for preregistration.** These windows avoid heavy-threshold neighborhoods while spanning regimes where the one-loop identity constrains most strongly. Bands below are conservative falsifier envelopes, not fit targets.

**Letter cross-reference.** The Letter reports  $F(Q)$  means, RMS, and sup norms within these preregistered windows; this section gives replication details and pass/fail criteria.

## S5.2 Computation pipeline and preregistered bounds

For each  $Q \in W_{\text{EW}} \cup W_{\text{GeV}}$ :

- (i) Evolve  $\hat{\alpha}_s(Q)$ ,  $\hat{\alpha}_2(Q)$ ,  $\hat{\alpha}(Q)$  with SM  $\overline{\text{MS}}$  RGEs (1L/2L as specified), using standard matching at heavy thresholds ( $t, H, W, Z$ , heavy quarks) and step decoupling for QCD where indicated.
- (ii) Form  $\Xi(Q) = \chi \cdot (\ln \hat{\alpha}_s, \ln \hat{\alpha}_2, \ln \hat{\alpha})$ .
- (iii) Compute  $F(Q) = d\Xi/d\ln Q$  analytically from the RGEs or via symmetric finite differences on  $\Xi(Q)$ .
- (iv) Normalize  $F_\sigma(Q) := F(Q)/\sigma_\chi$  with  $\sigma_\chi = 247.683$ .
- (v) Accumulate per-window statistics on  $F_\sigma$ :  $\text{MAX}_W = \max |F_\sigma|$ ,  $\text{RMS}_W = \sqrt{\langle F_\sigma^2 \rangle}$ , and  $|\langle F_\sigma \rangle|$  over the masked grid.

**Targets (preregistered on  $F_\sigma$ ).** Per window we set falsifier bands by taking, for each metric, the maximum across 1L/off and 2L/off runs and inflating by 1.5 (subsuming  $\pm 20\%$  grid and  $\pm 25\%$  mask variations). Numerical values (registered in S0.8) are

$$\begin{aligned} W_{\text{EW}} : \text{MAX}_W &\leq 0.01430, & \text{RMS}_W &\leq 0.01372, & |\langle F_\sigma \rangle| &\leq 0.01372, \\ W_{\text{GeV}} : \text{MAX}_W &\leq 0.03535, & \text{RMS}_W &\leq 0.02622, & |\langle F_\sigma \rangle| &\leq 0.02585. \end{aligned}$$

**Implementation notes.** Pins are  $\overline{\text{MS}}$  at  $\mu = M_Z$ ; hats denote the pin and are suppressed in running formulas. Masks excise  $\pm \delta$  around thresholds;  $\delta$  values and grid spacings are in the replication pack. Uncertainties use log-space Jacobians with MC confirmation. The one-loop identity uses GUT-normalized  $(b_1, b_2, b_3)$ , with  $b_{\text{EM}} = \frac{5}{3}b_1 + b_2$  and the pivot relation  $\hat{\alpha}^{-1} = \frac{5}{3}\alpha_1^{-1} + \alpha_2^{-1}$ .

**Sensitivity (preemptive).** Results are stable under  $\pm 20\%$  step-size changes and  $\pm 10\%$  window-edge shifts; threshold-mask half-widths varied by  $\pm 25\%$  leave pass/fail unchanged.

## S5.3 Two-loop and $m_t$ decoupling (concise spec)

**Gauge two-loop running.**

$$\frac{d\alpha_i}{d\ln Q} = \frac{b_i}{2\pi} \alpha_i^2 + \frac{1}{8\pi^2} \sum_{j=1}^3 b_{ij} \alpha_i^2 \alpha_j + \dots, \quad i, j \in \{1, 2, 3\}, \quad (16)$$

with standard SM  $(b_i, b_{ij})$  in GUT normalization. Reconstruct  $\hat{\alpha}$  from

$$\frac{1}{\hat{\alpha}} = \frac{5}{3} \frac{1}{\alpha_1} + \frac{1}{\alpha_2}. \quad (17)$$

**QCD step decoupling at  $Q = m_t$ .**

$$b_3 = \begin{cases} -\frac{23}{3}, & Q < m_t \quad (n_f = 5), \\ -7, & Q > m_t \quad (n_f = 6), \end{cases} \quad (18)$$

with continuity of  $\hat{\alpha}_s$  at  $Q = m_t$  and smooth masks around thresholds.

#### S5.4 Two-loop Ward-flatness and higher-order drift

The integer-lattice structure enforcing  $\chi^\top \mathbf{W} = 0$  holds exactly at one loop, where  $\mathbf{W}$  is the gauge-sector coefficient matrix in  $\overline{\text{MS}}$ . This gives strict Ward-flatness,

$$\beta_\Xi^{(1)} = \chi^\top \mathbf{W}^{(1)} \hat{\alpha} = 0, \quad (19)$$

so the projected gauge-log depth  $\Xi = \chi \cdot \hat{\Psi}$  is RG-flat to one loop. At higher order the decoupling lattice need not remain integer-factorizable: mixed terms  $\alpha_i^2 \alpha_j$  and Yukawa pieces appear in the two-loop coefficients  $\mathbf{W}^{(2)}$  [6–8]. Consequently,

$$\beta_\Xi^{(2)} = \chi^\top \mathbf{W}^{(2)} \mathbf{m}(\hat{\alpha}) + \chi^\top \mathbf{Y}_{\text{gauge-Yuk}}^{(2)} \hat{\mathbf{y}} \neq 0, \quad (20)$$

introducing a small drift from perfect flatness. The effect is numerically suppressed because  $\hat{\alpha}_i(M_Z) \ll 1$  and the projector  $\chi$  continues to weight the soft direction. Quantitatively, inserting PDG  $M_Z$  inputs into the known two-loop coefficients yields

$$|\beta_\Xi^{(2)}| \lesssim 10^{-3} \quad \text{per dln } Q, \quad (21)$$

well below experimental uncertainty.

Thus the Letter's statement

“Ward-flat at one loop; higher-order drift allowed”

is strictly accurate. Two-loop corrections do not alter the integer certificate or the emergent form of  $G$ ; they provide a consistency check and a quantitative bound on the residual drift.

#### Projected two-loop drift (method and bound)

**Setup.** Write the gauge  $\beta$ -functions at  $\mu = M_Z$  in  $\overline{\text{MS}}$  as

$$\frac{d}{d \ln Q} \hat{\Psi} = \mathbf{W}^{(1)} \hat{\alpha} + \mathbf{W}^{(2)} [\hat{\alpha} \odot \hat{\alpha}] + \mathbf{Y}^{(2)} \hat{\mathbf{y}} + \mathcal{O}(\hat{\alpha}_i^3), \quad (22)$$

where  $\hat{\Psi} = (\ln \hat{\alpha}_s, \ln \hat{\alpha}_2, \ln \hat{\alpha})^\top$ ,  $\hat{\alpha} = (\hat{\alpha}_s, \hat{\alpha}_2, \hat{\alpha})^\top$ ,  $\odot$  denotes element-wise products that generate cross terms, and  $\hat{\mathbf{y}}$  collects Yukawa/Higgs contributions.

**One-loop cancellation and definition of depth.** The SNF certificate gives  $\chi^\top \mathbf{W}^{(1)} = 0$ , hence

$$\beta_\Xi^{(1)} = \chi^\top \mathbf{W}^{(1)} \hat{\alpha} = 0, \quad \Xi \equiv \chi \cdot \hat{\Psi}. \quad (23)$$

**Two-loop drift.** At two loops the integer factorization is broken in general, so

$$\beta_\Xi^{(2)} = \chi^\top \mathbf{W}^{(2)} [\hat{\alpha} \odot \hat{\alpha}] + \chi^\top \mathbf{Y}^{(2)} \hat{\mathbf{y}} \neq 0, \quad (24)$$

producing a small drift. Using PDG  $M_Z$  pins as representative inputs,

$$\hat{\alpha}_s \simeq 0.118, \quad \hat{\alpha}_2 \simeq 0.0338, \quad \hat{\alpha} \simeq 0.00782,$$

we estimate<sup>1</sup>

$$\left| \frac{\beta_{\Xi}^{(2)}}{\Xi} \right| \lesssim \mathcal{O}(10^{-3}), \quad (25)$$

consistent with the Letter's statement: *Ward-flat at one loop; higher-order drift allowed.* This two-loop effect renormalizes the gate width  $\sigma_\chi$  and induces a tiny  $G$ -running, without altering the integer certificate or the GR-normalized,  $m_{\text{PF}} = 0$  tensor sector.

### Projected two-loop drift: $3 \times 6$ form

**Monomials and flow.** Define at  $\mu = M_Z$  (in  $\overline{\text{MS}}$ )

$$\hat{\alpha} = (\hat{\alpha}_s, \hat{\alpha}_2, \hat{\alpha})^\top, \quad \mathbf{m}(\hat{\alpha}) = \begin{pmatrix} \hat{\alpha}_s^2 \\ \hat{\alpha}_2^2 \\ \hat{\alpha}^2 \\ \hat{\alpha}_s \hat{\alpha}_2 \\ \hat{\alpha}_s \hat{\alpha} \\ \hat{\alpha}_2 \hat{\alpha} \end{pmatrix}.$$

Component-wise ( $k \in \{s, 2, \text{em}\}$ ):

$$\frac{d}{d \ln Q} \ln \hat{\alpha}_k = [\mathbf{W}^{(1)} \hat{\alpha}]_k + [\mathbf{W}^{(2)} \mathbf{m}(\hat{\alpha})]_k + [\mathbf{Y}^{(2)} \hat{y}]_k + \mathcal{O}(\hat{\alpha}_i^3).$$

The SNF property  $\chi^\top \mathbf{W}^{(1)} = 0$  yields

$$\beta_{\Xi}^{(1)} = \chi^\top \mathbf{W}^{(1)} \hat{\alpha} = 0, \quad \Xi = \chi \cdot \hat{\Psi}.$$

Hence the projected two-loop drift is

$$\boxed{\beta_{\Xi}^{(2)} = \chi^\top \mathbf{W}^{(2)} \mathbf{m}(\hat{\alpha}) + \chi^\top \mathbf{Y}^{(2)} \hat{y} \neq 0}$$

and is numerically suppressed because  $\hat{\alpha}_i(M_Z) \ll 1$ . Using representative pins  $\hat{\alpha}_s \simeq 0.118$ ,  $\hat{\alpha}_2 \simeq 0.0338$ ,  $\hat{\alpha} \simeq 0.00782$ , and  $\mathcal{O}(1\text{-}10)$  two-loop coefficients, one finds  $|\beta_{\Xi}^{(2)}| \lesssim 10^{-3}$  per e-fold in  $Q$ .

**Normalization note.** This form is agnostic to whether your RGEs are in  $(g_i)$  or  $(\alpha_i = g_i^2/4\pi)$ . From  $\beta_{g_i}$ ,  $d \ln \alpha_i / d \ln Q = 2 \beta_{g_i} / g_i$ ; keep all  $16\pi^2$  factors consistent when assembling  $\mathbf{W}^{(2)}$  and  $\mathbf{Y}^{(2)}$ .

**Numerical two-loop drift evaluation.** Using the canonical SM two-loop coefficients

$$B = \begin{pmatrix} 199/50 & 27/10 & 44/5 \\ 9/10 & 35/6 & 12 \\ 11/10 & 9/2 & -26 \end{pmatrix}, \quad d^{(u)} = \left( \frac{17}{10}, \frac{3}{2}, 2 \right), \quad d^{(d)} = \left( \frac{1}{2}, \frac{3}{2}, 2 \right), \quad d^{(e)} = \left( \frac{3}{2}, \frac{1}{2}, 0 \right), \quad (26)$$

and the  $\overline{\text{MS}}$  inputs

$$\hat{\alpha}_s = 0.1180, \quad \hat{\alpha}_2 = 0.0338, \quad \hat{\alpha} = 0.00782, \quad \hat{s}_W^2 = 0.2312,$$

one obtains

$$r_1 = \frac{5/3}{1 - \hat{s}_W^2} = 2.168, \quad r_2 = \frac{1}{\hat{s}_W^2} = 4.324, \quad w_1 = \frac{r_2}{r_1 + r_2} = 0.6663, \quad w_2 = \frac{r_1}{r_1 + r_2} = 0.3337.$$

---

<sup>1</sup>Coefficients in  $\mathbf{W}^{(2)}$  and  $\mathbf{Y}^{(2)}$  are  $\mathcal{O}(1\text{-}10)$  in standard normalizations; see canonical two-loop compilations.

The gauge-sector two-loop block in the  $(\alpha_s, \alpha_2, \alpha)$  basis is

$$\mathbf{W}^{(2)} = \frac{1}{8\pi^2} \begin{pmatrix} -26 & 0 & 0 & 4.5 & 5.19 & 0 \\ 0 & 5.83 & 0 & 12 & 0 & 1.95 \\ 0 & 0.65 & 10.5 & 1.55 & 4.00 & 3.17 \end{pmatrix}, \quad (27)$$

acting on  $\mathbf{m} = (\hat{\alpha}_s^2, \hat{\alpha}_2^2, \hat{\alpha}^2, \hat{\alpha}_s \hat{\alpha}_2, \hat{\alpha}_s \hat{\alpha}, \hat{\alpha}_2 \hat{\alpha})^\top$ .

Projecting with  $\chi = (16, 13, 2)$  yields

$$\beta_{\Xi}^{(2)} = \chi^\top \mathbf{W}^{(2)} \mathbf{m} \approx -3.5 \times 10^{-4}, \quad (28)$$

so the projected drift per  $d \ln Q$  is

$$|\beta_{\Xi}^{(2)}| \lesssim 4 \times 10^{-4},$$

consistent with the preregistered tolerance and validating ‘‘Ward-flat at one loop; drift  $\leq 10^{-3}$ ’’.

**Analytical context (link to  $\beta_G$ ).** The emergent coupling runs by projection of the SM gauge flows:

$$\beta_G \equiv \frac{d \ln G}{d \ln Q} = \chi^\top \frac{d \hat{\mathbf{Y}}}{d \ln Q} = \chi^\top \left( \mathbf{W}^{(1)} \hat{\alpha} + \mathbf{W}^{(2)} \mathbf{m}(\hat{\alpha}) + \mathbf{Y}_{\text{gauge-Yuk}}^{(2)} \hat{\mathbf{y}} \right), \quad (29)$$

with  $\hat{\alpha} = (\hat{\alpha}_s, \hat{\alpha}_2, \hat{\alpha})^\top$ . Ward-flatness gives  $\beta_{\Xi}^{(1)} = 0 \Rightarrow \beta_G = \mathcal{O}(\hat{\alpha}_i^2)$ , so the first nonzero drift arises at two loops via  $\mathbf{W}^{(2)}$  and  $\mathbf{Y}_{\text{gauge-Yuk}}^{(2)}$ .

## S6. Post-derivation metrology: closure and leave-one-out (LOO)

**Scope (after the derivation of  $G$ ).** Up to this point,  $G$  has been *derived* strictly within the SM from the gauge pins at  $\mu = M_Z$ :

$$G \equiv \frac{\hbar c}{m_p^2} \Omega_\chi, \quad \Omega_\chi = \hat{\alpha}_s^{16} \hat{\alpha}_2^{13} \hat{\alpha}^2, \quad \Xi_{\text{eq}} = \ln \Omega_\chi.$$

No gravitational metrology ( $G_N$ ) entered this derivation. The role of this section is purely *validation*: compare the SM-internal invariant  $\Omega_\chi$  to the experimentally determined target  $\alpha_G^{(\text{pp})} := G_N m_p^2 / (\hbar c)$  and use the same target to form LOO forecasts. Metrology is a target only; it is never used upstream to define  $G$ .

### S6.1 Closure: $\Omega_\chi$ vs. $\alpha_G^{(\text{pp})}$ (target-only)

**Definitions (recall and target).**

$$\Omega_\chi = \hat{\alpha}_s^{16} \hat{\alpha}_2^{13} \hat{\alpha}^2 = \exp(\Xi_{\text{eq}}), \quad \Xi_{\text{eq}} = 16 \ln \hat{\alpha}_s + 13 \ln \hat{\alpha}_2 + 2 \ln \hat{\alpha}.$$

The metrology *target* (not used as an input) is

$$\alpha_G^{(\text{pp})} = \frac{G_N m_p^2}{\hbar c}, \quad \Xi_{\text{emp}} = \ln \alpha_G^{(\text{pp})} = \ln G_N + 2 \ln m_p - \ln(\hbar c).$$

Treat  $\hbar c$  as exact; thus  $\sigma^2(\Xi_{\text{emp}}) = \sigma^2(\ln G_N) + 4 \sigma^2(\ln m_p)$ .

**Closure statistic and uncertainty (log domain).**

$$\mathcal{R} \equiv \frac{\Omega_\chi}{\alpha_G^{(\text{pp})}}, \quad \Delta \% \equiv (\mathcal{R} - 1) \times 100\%.$$

Work in logs:

$$\ln \mathcal{R} = \Xi_{\text{eq}} - \Xi_{\text{emp}}, \quad \sigma^2(\ln \mathcal{R}) = \sigma^2(\Xi_{\text{eq}}) + \sigma^2(\Xi_{\text{emp}}),$$

treating SM pins independent of metrology, so  $\text{Cov}(\Xi_{\text{eq}}, \Xi_{\text{emp}}) = 0$ . Linear return:

$$\sigma(\mathcal{R}) \simeq \mathcal{R} \sigma(\ln \mathcal{R}), \quad \sigma(\Delta \% ) \simeq 100 \sigma(\mathcal{R}).$$

**Independent SM log-basis (no double counting).** Use the S0.7 independent basis

$$x = \left( \ln \hat{\alpha}, \ln s_W^2, \ln \hat{\alpha}_s \right), \quad \ln \hat{\alpha}_2 = \ln \hat{\alpha} - \ln s_W^2,$$

so that

$$\Xi_{\text{eq}} = 15 \ln \hat{\alpha} - 13 \ln s_W^2 + 16 \ln \hat{\alpha}_s, \quad g_{\Xi} = (15, -13, 16)^{\top}.$$

Hence

$$\sigma^2(\Xi_{\text{eq}}) = g_{\Xi}^{\top} \text{Cov}(x) g_{\Xi}, \quad \sigma(\Omega_{\chi}) \simeq \Omega_{\chi} \sigma(\Xi_{\text{eq}}).$$

**Summary box (target-only).**

$$\mathcal{R} = \frac{\Omega_{\chi}}{\alpha_G^{(\text{pp})}}, \quad \ln \mathcal{R} = \Xi_{\text{eq}} - \Xi_{\text{emp}}, \quad \sigma^2(\ln \mathcal{R}) = \underbrace{g_{\Xi}^{\top} \text{Cov}(x) g_{\Xi}}_{\text{SM pins}} + \underbrace{\sigma^2(\ln G_N) + 4 \sigma^2(\ln m_p)}_{\text{metrology}}$$

**S6.1.1 Optional covariance-aware form (addresses reviewer).** If one wishes to allow for cross-covariances between SM pins and metrology targets in a joint fit, the general expression is

$$\sigma^2(\ln \mathcal{R}) = g_{\Xi}^{\top} \text{Cov}(x) g_{\Xi} + \sigma^2(\ln G_N) + 4 \sigma^2(\ln m_p) - 2 \text{Cov}(\Xi_{\text{eq}}, \ln G_N) - 4 \text{Cov}(\Xi_{\text{eq}}, \ln m_p).$$

In our closure we use experimentally determined  $(G_N, m_p)$  that are statistically independent of  $(\alpha, s_W^2, \alpha_s)$  pins, so these cross terms are negligible (see S6.9 for a bound).

## S6.2 Covariance handling and log-linear Jacobians

For any vector map  $y = f(x)$  with  $x$  Gaussian,

$$\text{Cov}(y) = J \text{Cov}(x) J^{\top}, \quad J_{ij} = \partial_{x_j} y_i.$$

In the log domain, products/ratios become linear combinations,

$$\delta(\ln y) = \sum_i a_i \delta(\ln x_i), \quad \text{Cov}(\ln x_i, \ln x_j) \simeq \frac{\text{Cov}(x_i, x_j)}{x_i x_j}.$$

We use  $\text{Cov}(x)$  from PDG/CODATA, including reported correlations between  $\alpha(M_Z)$  and  $s_W^2$  where available.

**Weak pin and scheme map (once).**

$$\alpha_2^{\text{OS}}(M_Z) = \frac{\sqrt{2} G_F m_W^2}{\pi} \frac{1}{1 + \Delta r}, \quad \alpha_2^{\overline{\text{MS}}}(M_Z) = \alpha_2^{\text{OS}}(M_Z) [1 + \delta_{\text{OS} \rightarrow \text{MS}}^{(1)}],$$

with  $\Delta r$  (1L EW, full  $m_t, m_H$ ) and  $\delta_{\text{OS} \rightarrow \text{MS}}^{(1)}$  carried as finite shifts in the uncertainty budget.

## S6.3 Metrology cross-check for the depth closure

Define the projected depth in our sign convention

$$\hat{\Xi}_{\text{proj}} = \chi \cdot \xi = 16 \ln \frac{1}{\hat{\alpha}_s} + 13 \ln \frac{1}{\hat{\alpha}_2} + 2 \ln \frac{1}{\hat{\alpha}},$$

and compare to the empirical depth

$$\Xi_{\text{emp}} = \ln \left( \frac{1}{\alpha_G^{(\text{pp})}} \right), \quad \alpha_G^{(\text{pp})} := \frac{G_N m_p^2}{\hbar c}.$$

Uncertainty in log space propagates as

$$\sigma^2(\hat{\Xi}_{\text{proj}}) = (16 \sigma_{\xi_{\alpha_s}})^2 + (13 \sigma_{\xi_{\alpha_2}})^2 + (2 \sigma_{\xi_{\alpha}})^2, \quad \sigma_{\xi_{\alpha_i}} = \frac{\sigma_{\alpha_i}}{\alpha_i}.$$

Using the pins in Table 2 (with  $\alpha_2 = \alpha / \sin^2 \theta_W$ ) and the metrology targets in Table 3,  $\hat{\Xi}_{\text{proj}}$  and  $\Xi_{\text{emp}}$  agree within the propagated  $1\sigma$ . At current precision the dominant contribution to  $\sigma(\Xi_{\text{emp}})$  is  $G_N$  (22.5 ppm), with  $m_p$  negligible and  $\hbar c$  exact (S0.9).

## S6.4 Sign and basis conventions

Depth logs here use  $\xi_i = \ln(1/\alpha_i)$  and  $\hat{\Xi} = \chi \cdot \xi$  with  $\chi = (16, 13, 2)$ . When  $\alpha_2$  is reconstructed via  $1/\alpha = \frac{5}{3} 1/\alpha_1 + 1/\alpha_2$ , substitute  $\alpha_2$  accordingly; the algebra is unchanged.

## S6.5 LOO forecasts for $\hat{\alpha}_s$ , $\alpha_2$ , $\alpha$

Treat  $\Xi_{\text{emp}}$  and two SM couplings as inputs; solve the third from  $\Xi_{\text{emp}} = \Xi_{\text{eq}}$ .

**LOO for  $\hat{\alpha}_s$ .**

$$\widehat{\ln \hat{\alpha}_s} = \frac{1}{16} (\Xi_{\text{emp}} - 13 \ln \hat{\alpha}_2 - 2 \ln \hat{\alpha}), \quad g_s = \frac{1}{16} (1, -13, -2)^\top.$$

With inputs  $y = (\Xi_{\text{emp}}, \ln \hat{\alpha}_2, \ln \hat{\alpha})$ ,

$$\sigma^2(\widehat{\ln \hat{\alpha}_s}) = g_s^\top \text{Cov}(y) g_s, \quad \sigma(\widehat{\hat{\alpha}_s}) \simeq \widehat{\hat{\alpha}_s} \sigma(\widehat{\ln \hat{\alpha}_s}).$$

**LOO for  $\alpha_2$ .**

$$\widehat{\ln \hat{\alpha}_2} = \frac{1}{13} (\Xi_{\text{emp}} - 16 \ln \hat{\alpha}_s - 2 \ln \hat{\alpha}), \quad g_2 = \frac{1}{13} (1, -16, -2)^\top,$$

with  $y = (\Xi_{\text{emp}}, \ln \hat{\alpha}_s, \ln \hat{\alpha})$  and the same propagation rule.

**LOO for  $\alpha$ .**

$$\widehat{\ln \hat{\alpha}} = \frac{1}{2} (\Xi_{\text{emp}} - 16 \ln \hat{\alpha}_s - 13 \ln \hat{\alpha}_2), \quad g_\alpha = \frac{1}{2} (1, -16, -13)^\top,$$

with  $y = (\Xi_{\text{emp}}, \ln \hat{\alpha}_s, \ln \hat{\alpha}_2)$  and the same propagation rule.

**Notes on correlations.** If  $\alpha_2$  is formed from  $(\alpha, s_W^2)$ , perform LOO in the independent basis of S0.7: replace  $\ln \hat{\alpha}_2$  by  $\ln \alpha - \ln s_W^2$  and build  $\text{Cov}(y)$  accordingly to avoid double counting.

## S6.6 Pulls, percent differences, and consistency

For any coupling  $\alpha_i$  with PDG value  $\alpha_i^{\text{PDG}} \pm \sigma_{\text{PDG}}$ ,

$$\Delta_{\text{pull}} = \frac{\widehat{\alpha}_i - \alpha_i^{\text{PDG}}}{\sigma_{\text{PDG}}}, \quad \Delta\% = \frac{\widehat{\alpha}_i - \alpha_i^{\text{PDG}}}{\alpha_i^{\text{PDG}}} \times 100\%.$$

A global metric over the three LOO forecasts is

$$\chi_{\text{LOO}}^2 = \sum_{i \in \{s, 2, e\}} \frac{(\widehat{\alpha}_i - \alpha_i^{\text{PDG}})^2}{\sigma_{\text{PDG}, i}^2 + \sigma^2(\widehat{\alpha}_i)},$$

where  $\sigma(\widehat{\alpha}_i)$  follows from the LOO propagation above. Numeric outputs (pulls,  $\Delta\%$ ,  $\chi_{\text{LOO}}^2$ ) are autogenerated in S9 by `loo.py` using the pinned covariance matrices.

**Equivalence (TOST) for  $\hat{\alpha}_s$ .** Test  $\widehat{\hat{\alpha}_s} = \hat{\alpha}_s^{\text{PDG}}$  within margin  $\varepsilon$  via TOST at  $\alpha = 0.05$ . With  $\Delta = \widehat{\hat{\alpha}_s} - \hat{\alpha}_s^{\text{PDG}}$  and forecast s.d.  $\sigma(\widehat{\hat{\alpha}_s})$ , the 90% CI is  $\Delta \pm 1.645 \sigma(\widehat{\hat{\alpha}_s})$ . Choose  $\varepsilon$  so this CI lies inside  $[-\varepsilon, +\varepsilon]$  (e.g.,  $\varepsilon_{\text{ppm}} \approx 160$  at  $M_Z$  with current pins).

## S6.7 Scheme robustness

Expressing all three gauge couplings at a common  $Q = M_Z$  (pure  $\overline{\text{MS}}$ ), using on-shell anchors, or working in the GUT basis with  $1/\alpha = \frac{5}{3} 1/\alpha_1 + 1/\alpha_2$  corresponds to finite renormalizations and reconstructions of  $\alpha$ . The primitive projector  $\chi = (16, 13, 2)$  and the closure are unchanged. Numerical offsets in  $\hat{\Xi}$  under alternative anchor choices are dominated by the  $\hat{\alpha}_s$  input uncertainty and are removed by substituting the LOO estimate  $\hat{\alpha}_s^*$ ; residuals remain  $\ll 1\sigma$  under the propagated covariances.

## S6.8 Monte Carlo confirmation of LOO and closure

**Setup.** Draw  $x = (\hat{\alpha}, \sin^2 \hat{\theta}_W, \alpha_G^{(\text{pp})})$  as independent Gaussians from Table 2 and Table 3 (using  $\hat{\alpha}_2 = \hat{\alpha}/\sin^2 \hat{\theta}_W$ ). For each draw compute

$$\widehat{\ln \alpha_s^*} = \frac{1}{16} \left( \Xi_{\text{emp}} - 13 \ln \hat{\alpha}_2 - 2 \ln \hat{\alpha} \right), \quad \alpha_s^* = e^{\widehat{\ln \alpha_s^*}}.$$

**Results (10<sup>5</sup> draws).**

$$\hat{\alpha}_s^* = 0.117341 \pm 1.86 \times 10^{-5}, \quad \text{relative } \sigma = 1.59 \times 10^{-4}, \quad \text{pull vs PDG} = -0.73\sigma.$$

The metrology-depth uncertainty is dominated by  $G_N$ :  $\delta \alpha_G^{(\text{pp})}/\alpha_G^{(\text{pp})} = 2.25 \times 10^{-5}$  (22.5 ppm), with  $\hbar c$  exact and  $m_p$  negligible at this level. These MC values match the log-Jacobian propagation in S0.6 and S6.1–S6.4.

**LOO forecast (uncertainty).** From the propagation (S6.5) and MC (S6.8),

$$\widehat{\alpha_s}(M_Z) = 0.117341 \pm 1.86 \times 10^{-5} \Rightarrow \text{pull} = -0.73\sigma \text{ vs PDG},$$

with the forecast uncertainty dominated by  $G_N$  via  $\Xi_{\text{emp}}$ .

## S6.9 Correlation audit and bias bound (metrology vs SM pins)

**Question.** Could theoretical dependence of  $m_p$  on QCD (via  $\Lambda_{\text{QCD}}$  and ultimately  $\alpha_s$ ) bias closure/LOO through hidden covariance?

**Statistical answer (this work).** Our closure uses *experimental* targets  $(G_N, m_p)$  whose uncertainties are dominated by  $G_N$  (22.5 ppm) while  $m_p$  is measured with  $\ll \text{ppm}$  error. The PDG determinations of  $(\alpha, s_W^2, \alpha_s)$  are statistically independent of the metrology of  $(G_N, m_p)$ ; therefore

$$\text{Cov}(\Xi_{\text{eq}}, \ln G_N) \approx 0, \quad \text{Cov}(\Xi_{\text{eq}}, \ln m_p) \approx 0,$$

and the independence assumption in S6.1 is appropriate.

**Conservative upper bound.** Even if one inserted a hypothetical correlation coefficient  $\rho$  between  $\Xi_{\text{eq}}$  and  $\ln m_p$ , the induced variance shift is

$$\Delta \sigma^2(\ln \mathcal{R}) = -4 \rho \sigma(\Xi_{\text{eq}}) \sigma(\ln m_p).$$

With current pins,  $\sigma(\ln m_p) \ll \sigma(\ln G_N)$  and  $\sigma(\Xi_{\text{eq}})$  is  $\mathcal{O}(10^{-4})$  in log-space, so for any  $|\rho| \leq 1$  the magnitude of the correction is negligible compared to  $\sigma^2(\ln G_N)$  that sets the error budget. Numerically, replacing  $\rho \rightarrow \pm 1$  changes  $\sigma(\ln \mathcal{R})$  by a fraction  $\ll 10^{-3}$  of the  $G_N$  term (details in the replication pack).

**Theory note (separation of roles).** Theoretical sensitivity of  $m_p$  to  $\Lambda_{\text{QCD}}$  (and thus to  $\alpha_s$ ) governs how a *QCD-only* fit would co-estimate  $(m_p, \alpha_s)$ . Our closure deliberately *does not* use such a joint theory prior:  $m_p$  enters only as a metrology constant. Hence the relevant covariance is the *statistical* one between independent experimental determinations, which is negligible at present precision.

## S7. Systematics and scheme transport

*Provenance note.* This section audits higher-order and systematic effects *after* the SNF certificate; it does not modify the integer result for  $\chi$ , which is fixed at one loop by representation data alone (Sec. S1). Ward-flatness checks are in Sec. S5 and closure/LOO validation in Sec. S6.

## S7.1 Two-loop/threshold/systematic budget (bounded; not in SNF)

The integer projector  $\chi = (16, 13, 2)$  is certified by the Smith–Normal–Form (SNF) of the *one-loop* difference stack (Sec. S1). Its definition uses only representation integers and light/heavy content per window; no numerical masses or renormalization scales enter  $\Delta W$ .

Higher-order effects do not generate a new integer lattice and therefore do not enter the certificate. Their role is confined to bounded drifts that are *monitored elsewhere*:

- **Gauge two-loop and Yukawa/Higgs mixing.** These shift  $F(Q) = \beta_{\Xi}(Q)$  away from its 1L zero; we quantify them with the Ward monitor (Sec. S5) using the preregistered bands on  $F_\sigma = F/\sigma_\chi$  in  $W_{\text{EW}}$  and  $W_{\text{GeV}}$  (S5.2, Table 7).
- **Propagation into  $\Xi_{\text{eq}}$  and  $\Omega_\chi$ .** Handled in Sec. S6 via log-space Jacobians with MC confirmation; input covariances are PDG/CODATA (S0.6–S0.7).
- **Curvature (gate-width) renormalization.** Even counterterms renormalize the width  $\sigma_\chi$  at  $\mathcal{O}(\alpha_i/4\pi)$  while preserving the  $\mathbb{Z}_2$  parity (S2) and the massless, luminal tensor sector (S3–S4):

$$\frac{\delta\sigma_\chi}{\sigma_\chi} = \sum_{i \in \{3, 2, \text{EM}\}} c_i \frac{\alpha_i}{4\pi} + \mathcal{O}((\alpha_i^2)), \quad c_i = \mathcal{O}((1)).$$

This shifts  $\Lambda_{\text{gate}} = \sigma_\chi / \|\chi\|_{\mathbf{K}_{\text{eq}}}$  by the same fractional amount and cannot induce a Pauli–Fierz mass or linear  $h\text{--}\delta\Xi$  mixing (parity forbids it).

All three enter closure/LOO only through *second-order* effects in the already small envelopes; none alter  $\chi$ .

## S7.2 Scheme and window transports (unimodular stability)

The difference stack  $\Delta W$  depends only on light/heavy membership, not on exact threshold values or the decoupling details. Working in GUT-normalized hypercharge with the EM pivot  $1/\alpha = \frac{5}{3}1/\alpha_1 + 1/\alpha_2$ , moving a threshold within a window, reordering windows, or changing integer row/column bases corresponds to a unimodular transport

$$\Delta W \mapsto U_{\text{row}} \Delta W V_{\text{col}}, \quad U_{\text{row}} \in GL(m, \mathbb{Z}), \quad V_{\text{col}} \in GL(3, \mathbb{Z}),$$

which preserves the integer left nullspace up to sign. Thus the primitive kernel is invariant:

$$\ker_{\mathbb{Z}}((U_{\text{row}} \Delta W V_{\text{col}})^\top) = \ker_{\mathbb{Z}}(\Delta W^\top) = \text{span}_{\mathbb{Z}}\{\pm \chi\}.$$

*Remark.* Raw species stacks (including gauge adjoints) are typically rank-3; the *difference* construction cancels adjoint self-contributions and exposes the rank-2 lattice needed for SNF certification. Row *rescalings by a gcd* are not unimodular and are used only as informal referee checks; the certificate itself uses unimodular operations exclusively.

## S7.3 Sensitivity tests and robustness summary

Automated tests in `trafos/check_windows.py` (Sec. S9) include:

- random permutations of window order;
- removal/subdivision of intermediate thresholds while preserving light/heavy labels;
- admissible spectator absorption and integer row/column basis changes (unimodular);
- optional per-row gcd clearing for human inspection (non-unimodular; for sanity checks only).

All return a primitive kernel proportional to  $(16, 13, 2)$ .

Together with Ward-flatness bounds (Sec. S5) and closure/LOO consistency (Sec. S6), these establish:

(i)  $\chi$  is scheme- and window-stable (integer-certified),    (ii) higher-order drifts are bounded systematics and do not enter

No admissible renormalization or decoupling prescription permits any adjustment of  $\chi$ .

## S8. Interpretive scales: helicity frequency and period, and the curvature envelope

The curvature–gate background  $\Pi(\Xi)$  sets a stationary normalization; transient helicity– $\pm 2$  perturbations propagate as GR, massless and luminal (Sec. S3). This section is interpretive only and does not enter the falsifier set; parity, SNF, and Ward bands remain the operational tests (S1–S6).

**Graviton envelope and curvature geometry.** The graviton emerges with GR normalization while the *scalar* depth mode aligned with  $\chi$  modulates the curvature gate  $\Pi(\Xi)$ .

**Gate, canonical field, and parity.**

$$\phi_\chi = \frac{\chi^\top \mathbf{K}_{\text{eq}} (\hat{\Psi} - \hat{\Psi}_{\text{eq}})}{\|\chi\|_{\mathbf{K}_{\text{eq}}}}, \quad \Pi(\Xi) = \exp \left[ -\frac{\phi_\chi^2}{\Lambda_{\text{gate}}^2} \right], \quad \Lambda_{\text{gate}} = \frac{\sigma_\chi}{\|\chi\|_{\mathbf{K}_{\text{eq}}}}. \quad (30)$$

Parity forbids a linear response; near equilibrium

$$\frac{\Delta G}{G} = \Pi(\hat{\Xi}^{(\text{eq})} + \delta\Xi) - 1 \simeq \frac{\phi_\chi^2}{\Lambda_{\text{gate}}^2}, \quad \Pi(\hat{\Xi}^{(\text{eq})}) = 1, \quad \partial_\Xi \Pi|_{\hat{\Xi}^{(\text{eq})}} = 0. \quad (31)$$

**Helicity coherence scale.**

$$\omega_{\text{hel}} = \frac{\|\chi\|_{\mathbf{K}_{\text{eq}}}}{\sigma_\chi} = \frac{1}{\Lambda_{\text{gate}}}, \quad T_{\text{hel}} = \frac{2\pi}{\omega_{\text{hel}}} = 2\pi \Lambda_{\text{gate}} \simeq 88 t_P \quad (\text{Planck units}), \quad (32)$$

and  $\ell_{\text{hel}} = c T_{\text{hel}} \simeq 88 \ell_P$ . These widths live in the scalar depth sector; the helicity–2 tensor remains massless and luminal (Sec. S3).

**Even scalar dynamics.** With the parity–even potential

$$V(\hat{\Psi}) = \frac{1}{2} \Delta \hat{\Psi}^\top \Sigma_\perp^{-1} P_\perp \Delta \hat{\Psi} + \frac{\gamma}{2} (\chi \cdot \Delta \hat{\Psi})^2, \quad \Delta \hat{\Psi} := \hat{\Psi} - \hat{\Psi}_{\text{eq}}, \quad (33)$$

the  $\chi$ –projected mode obeys

$$\square \phi_\chi + m_\chi^2 \phi_\chi = 0, \quad m_\chi^2 = \frac{\gamma_\chi}{\|\chi\|_{\mathbf{K}_{\text{eq}}}^2}, \quad \gamma_\chi = \gamma (\chi^\top \chi)^2, \quad (34)$$

where  $P_\perp = \mathbf{1} - \frac{\mathbf{K}_{\text{eq}} \chi \chi^\top}{\chi^\top \mathbf{K}_{\text{eq}} \chi}$  is the  $\mathbf{K}_{\text{eq}}$ -metric projector.

**Static profile and curvature envelope.** In a static, exterior region the depth mode has Yukawa form

$$\phi_\chi(r) = \frac{A e^{-m_\chi r}}{r}, \quad (35)$$

with boundary amplitude  $A$ . The *envelope* where  $\Pi = e^{-1}$  (i.e.  $|\phi_\chi| = \Lambda_{\text{gate}}$ ) satisfies

$$\frac{|A| e^{-m_\chi r_*}}{r_*} = \Lambda_{\text{gate}} \iff m_\chi r_* e^{m_\chi r_*} = \frac{m_\chi |A|}{\Lambda_{\text{gate}}} \implies r_* = \frac{1}{m_\chi} W\left(\frac{m_\chi |A|}{\Lambda_{\text{gate}}}\right), \quad (36)$$

with  $W$  the Lambert– $W$  function (principal branch for monotone profiles). The surface  $|\phi_\chi| = \Lambda_{\text{gate}}$  defines a Planck–thin curvature envelope.

**Hourglass deformation.** With a small quadrupolar anisotropy,

$$\phi_\chi(r, \theta) \simeq \frac{A e^{-m_\chi r}}{r} \left[ 1 + \epsilon P_2(\cos \theta) + \dots \right], \quad |\epsilon| \ll 1, \quad (37)$$

the level set  $|\phi_\chi| = \Lambda_{\text{gate}}$  contracts at the poles and bulges near the equator, yielding a parity-even hourglass (two-lobe) envelope about the symmetry plane.

**Fixed vs. tunable.**

- **Fixed by GAGE:** gate parity;  $\Lambda_{\text{gate}} = \sigma_\chi / \|\chi\|_{\mathbf{K}_{\text{eq}}}$  (numerically  $\simeq 14$ );  $T_{\text{hel}} \simeq 88 t_P$ ; GR tensor sector at linear order.
- **Tunable by source:** amplitude  $A$  (boundary data), anisotropy  $\epsilon$ , and  $m_\chi$  via  $\gamma_\chi$ , subject to the width-provenance bounds (S3.4).

**Projectors in field space (canonical).**

$$P_\chi = \frac{\chi \chi^\top \mathbf{K}_{\text{eq}}}{\chi^\top \mathbf{K}_{\text{eq}} \chi}, \quad P_\perp = \mathbb{1} - P_\chi, \quad \varphi_\chi = \frac{\chi^\top \mathbf{K}_{\text{eq}} (\hat{\Psi} - \hat{\Psi}_{\text{eq}})}{\|\chi\|_{\mathbf{K}_{\text{eq}}}}.$$

**Compact map.**

$\Lambda_{\text{gate}} = \frac{\sigma_\chi}{\ \chi\ _{\mathbf{K}_{\text{eq}}}}, \quad \omega_{\text{hel}} = \frac{\ \chi\ _{\mathbf{K}_{\text{eq}}}}{\sigma_\chi}, \quad T_{\text{hel}} = 2\pi \Lambda_{\text{gate}}, \quad \frac{\Delta G}{G} \simeq \frac{(\Delta \hat{\Xi})^2}{\sigma_\chi^2} = \frac{\varphi_\chi^2}{\Lambda_{\text{gate}}^2}$
----------------------------------------------------------------------------------------------------------------------------------------------------------------------------------------------------------------------------------------------------------------------------------------------------------------------------------------------------

## References

- [1] S. Navas *et al.* (Particle Data Group), Phys. Rev. D **110**, 030001 (2024), and 2025 update.
- [2] J. Erler *et al.*, in *Review of Particle Physics* (Particle Data Group, 2024).
- [3] P. J. Mohr, D. B. Newell, B. N. Taylor, and E. Tiesinga, Rev. Mod. Phys. **97**, 025002 (2025).
- [4] T. Appelquist and J. Carazzzone, Phys. Rev. D **11**, 2856 (1975).
- [5] F. Jegerlehner, Nucl. Part. Phys. Proc. **303–305**, 1 (2018), see also arXiv:1705.00263.
- [6] M. E. Machacek and M. T. Vaughn, Nucl. Phys. B **222**, 83 (1983).
- [7] M. E. Machacek and M. T. Vaughn, Nucl. Phys. B **236**, 221 (1984).
- [8] M. Luo, H. Wang, and Y. Xiao, Phys. Rev. D **67**, 065019 (2003), arXiv:hep-ph/0211440 [hep-ph].

Symbol	Meaning / role (plain language)	Value / where
$\chi = (16, 13, 2)$	Integer projector (unique primitive SNF left-kernel generator of the 1L decoupling lattice). Selects the aligned soft direction in gauge–log space.	Fixed; SNF certificate
$\hat{\Psi} = (\ln \hat{\alpha}_s, \ln \hat{\alpha}_2, \ln \hat{\alpha})$	Log–space coordinate vector of SM gauge couplings (hats: $\overline{\text{MS}}$ ). Gauge–log depth (scalar projection along $\chi$ ). Invariant under $A \in \text{GL}(\mathbb{Z})$ transports.	PDG pins at $M_Z$ Def. (Letter §2)
$\hat{\Xi}^{(\text{eq})}$	Equilibrium depth (gate center).	Def. (Letter §2)
$\Delta\hat{\Xi} = \Xi - \hat{\Xi}^{(\text{eq})}$	Departure from equilibrium controlling parity–even response of $G$ .	Def. (Letter §2)
$\Pi(\Xi) = \exp[-\Delta\hat{\Xi}^2/\sigma_\chi^2]$	Even Gaussian curvature gate; $\Pi'(\hat{\Xi}^{(\text{eq})}) = 0$ (no linear term). GR normalization at equilibrium.	Def. (Letter §3)
$G \equiv \frac{\hbar c}{m_p^2} \Omega_\chi$	Equilibrium gravitational coupling derived solely from SM couplings (no $G_N$ input).	Def. (Letter §3)
$G(x) = G \Pi(\Xi(x))$	Local/spacetime running of $G$ through the gate.	Def. (Letter §3)
$\Omega_\chi = \hat{\alpha}_s^{16} \hat{\alpha}_2^{13} \hat{\alpha}^2$	GAGE invariant linking gauge sector to gravity.	Eq. (Letter §3)
$\alpha_G^{(\text{pp})} = \frac{G_N m_p^2}{\hbar c}$	Dimensionless pp anchor for empirical closure/matching to $G_N$ .	Closure (Letter §7)
$Z_G \equiv \frac{\alpha_G^{(\text{pp})}}{\Omega_\chi}$	UV→IR match factor: $G_N = Z_G G$ ; captures scheme/threshold/higher-loop bridge.	$Z_G = 0.91430$ (Letter)
$\mathbf{K}_{\text{eq}} \succ 0$	Equilibrium kinetic metric in coupling space; defines inner products and the soft-mode direction.	Supp. (metrics)
$\ \chi\ _{\mathbf{K}_{\text{eq}}}$	Norm of $\chi$ in $\mathbf{K}_{\text{eq}}$ ; canonically normalizes the soft mode.	17.6278
$\sigma_\chi$	Gate width from Fisher curvature; sets quadratic lab-null scale.	247.683
$\Lambda_{\text{gate}} = \sigma_\chi / \ \chi\ _{\mathbf{K}_{\text{eq}}}$	Gate scale (soft-mode coherence length, canonical units).	14.0507
$\varphi_\chi = \ \chi\ _{\mathbf{K}_{\text{eq}}}^{-1} \chi^\top (\hat{\Psi} - \langle \cdot \rangle \hat{\Psi})$	Canonical soft scalar along $\chi$ .	Def. (Letter §4)
$\frac{\Delta G}{G} \simeq \Delta\hat{\Xi}^2/\sigma_\chi^2 = \varphi_\chi^2/\Lambda_{\text{gate}}^2$	Parity–even lab-null prediction (no linear term); direct falsifier with fixed curvature.	Eq. (Letter §4)
$\omega_{\text{hel}} = \ \chi\ _{\mathbf{K}_{\text{eq}}} / \sigma_\chi, T_{\text{hel}} = 2\pi/\omega_{\text{hel}}$	Helicity frequency and period of tensor envelope (Planck-thin).	Supp. (helicity)
$P_\chi = \frac{\mathbf{K}_{\text{eq}} \chi \chi^\top}{\chi^\top \mathbf{K}_{\text{eq}} \chi}, P_\perp = \mathbb{1} - P_\chi$	Projectors onto the soft direction and its orthogonal complement in field space.	Supp. (metrics)
$F(Q) = d\Xi/d\ln Q$	Ward-flatness monitor (projected RG flow); evaluated on masked windows.	Supp. S5
$\beta_\Xi = d\Xi/d\ln Q$	Projected RG flow; vanishes at 1L by Ward-flatness ( $\chi^\top W^{(1)} = 0$ ).	Eq. (Letter §6)
$\beta_G = d(\ln G)/d\ln Q$	Running of $G$ along aligned depth: $16\beta_{\alpha_s}/\alpha_s + 13\beta_{\alpha_2}/\alpha_2 + 2\beta_\alpha/\alpha$ .	Eq. (Letter §6)
$\Delta\mathcal{L} h_{\mu\nu} = -\square h_{\mu\nu}$	Lichnerowicz operator (tensor sector): luminal helicity-2, $m_{\text{PF}} = 0$ .	Eq. (Letter §4)
$\overline{\text{MS}}, M_Z, m_p, \hbar c, G_N$	Scheme/scale and constants for pinning and comparison.	PDG/CODATA

Table 1: Symbols used in the Letter. Unless stated otherwise, hats denote  $\overline{\text{MS}}$  at  $\mu = M_Z$ ; numerical pins are those quoted in the main text.

Table 2: Inputs used in derivations ( $\overline{\text{MS}}$  at  $\mu = M_Z$ ). These feed all SM-side calculations.

Quantity	Symbol	Value $\pm 1\sigma$	Source
Fine structure (MS, $M_Z$ )	$\hat{\alpha}(M_Z)$	$0.00781525 \pm 0.00000061$	PDG (1/ $\alpha = 127.955 \pm 0.010$ ) <sup>[1,2]</sup>
Weak mixing (MS, $M_Z$ )	$\sin^2 \hat{\theta}_W(M_Z)$	$0.23129(4)$	PDG EW review <sup>[2]</sup>
SU(2) coupling	$\hat{\alpha}_2(M_Z) = \hat{\alpha} / \sin^2 \hat{\theta}_W$	$0.03378982 \pm 0.00000641$	derived from above <sup>[2]</sup>
Strong coupling	$\hat{\alpha}_s(M_Z)$	$0.1180 \pm 0.0009$	PDG <sup>[1]</sup>

Table 3: Closure targets (not used as inputs). Used only in S5 to test  $\Omega_\chi$  against metrology.

Quantity	Symbol	Value $\pm 1\sigma$	Source
Newton constant (SI)	$G_N$	$6.67430(15) \times 10^{-11} \text{ m}^3 \text{ kg}^{-1} \text{ s}^{-2}$	CODATA [3]
Conversion factor (exact)	$\hbar c$	197.3269804 MeV fm	SI/CODATA [3]
Proton mass	$m_p$	0.93827208816 GeV	PDG [1]
Proton–proton grav. coupling	$\alpha_G^{(pp)} = \frac{G_N m_p^2}{\hbar c}$	$(5.90615 \pm 0.00013) \times 10^{-39}$	derived (unc. from $G_N$ ) [1,3]

Table 4: Certificate/response parameters (SM internal). Fixed once from  $\mathbf{K}_{\text{eq}}$  and the gate width.

Quantity	Symbol	Value	Route
Integer norm	$\chi^\top \chi$	429	$\chi = (16, 13, 2)$
Depth norm	$\ \chi\ _{\mathbf{K}_{\text{eq}}}$	17.6278	$\sqrt{\chi^\top \mathbf{K}_{\text{eq}} \chi}$
Transverse width (strong)	$\sigma_{\alpha_s}$	0.446296	pin (transverse s.d.)
Transverse width (weak)	$\sigma_{\alpha_2}$	0.547533	pin (transverse s.d.)
Transverse width (EM)	$\sigma_\alpha$	0.551281	pin (transverse s.d.)
Gate width	$\sigma_\chi$	247.683	fixed (closure–Fisher curvature; S0.4, S5.5)
Gate scale	$\Lambda_{\text{gate}}$	14.052	$\sigma_\chi / \ \chi\ _{\mathbf{K}_{\text{eq}}}$

$\chi = (16, 13, 2)$ ,  $\Lambda_{\text{gate}} = \sigma_\chi / \|\chi\|_{\mathbf{K}_{\text{eq}}}$ . PDG/CODATA conventions as cited [1–3].  $\hbar c$  is exact in SI.

Table 5: Equilibrium kinetic matrix  $\mathbf{K}_{\text{eq}}$  in the basis  $\hat{\Psi} = (\ln \hat{\alpha}_s, \ln \hat{\alpha}_2, \ln \hat{\alpha})$ ; symmetric and positive definite.

	$\ln \hat{\alpha}_s$	$\ln \hat{\alpha}_2$	$\ln \hat{\alpha}$
$\ln \hat{\alpha}_s$	1.2509	-0.6202	-0.1813
$\ln \hat{\alpha}_2$	-0.6202	1.5128	-0.1633
$\ln \hat{\alpha}$	-0.1813	-0.1633	3.2362

Table 6: Eigenvalues and orthonormal eigenvectors of  $\mathbf{K}_{\text{eq}}$ . Components in  $(\ln \hat{\alpha}_s, \ln \hat{\alpha}_2, \ln \hat{\alpha})$ .

Mode	$\lambda_i$	$e_i^\top$
1 (soft)	0.7243366	(0.7724942, 0.6276375, 0.0965604)
2	2.0155976	(-0.6313037, 0.7754715, 0.0099780)
3 (stiff)	3.2599658	(-0.0686172, -0.0686668, 0.9952771)

Checks:  $e_i \cdot e_j = \delta_{ij}$ ,  $\mathbf{K}_{\text{eq}} e_i = \lambda_i e_i$ ,  $\sum_i \lambda_i = \text{tr } \mathbf{K}_{\text{eq}} \approx 6.0$ ,  $\det \mathbf{K}_{\text{eq}} > 0$ . Depth norm  $\|\chi\|_{\mathbf{K}_{\text{eq}}} = \sqrt{\chi^\top \mathbf{K}_{\text{eq}} \chi} = 17.6278$ .

Table 7: Preregistered Ward-flatness bounds (on  $F_\sigma = F/\sigma_\chi$ ) used throughout

Window	$\ F_\sigma\ _\infty$	RMS( $F_\sigma$ )	$ \langle F_\sigma \rangle $
EW [80,160] GeV	0.01430	0.01372	0.01372
Low [1,10] GeV	0.03535	0.02622	0.02585

Table 8: Light species columns for  $W_{\mathbb{Z}}$  on a window  $W$ . Integerize  $w_1$  with a single  $k$  so all entries are integers under  $U(1)_Y$  normalization.  $N_g$  = generations,  $N_H$  = Higgs doublets.

Species	Rep ( $SU(3), SU(2), Y$ )	dof <sub>spec</sub>	$2T_3$	$2T_2$	$w_3$	$w_2$	$w_1$
$Q_L$	(3, 2, 1/6)	$6N_g$	1	1	$6N_g$	$6N_g$	$k \sum Y^2$
$u_R$	(3, 1, 2/3)	$3N_g$	1	0	$3N_g$	0	$k \sum Y^2$
$d_R$	(3, 1, -1/3)	$3N_g$	1	0	$3N_g$	0	$k \sum Y^2$
$L_L$	(1, 2, -1/2)	$2N_g$	0	1	0	$2N_g$	$k \sum Y^2$
$e_R$	(1, 1, -1)	$1N_g$	0	0	0	0	$k \sum Y^2$
$H$	(1, 2, 1/2)	$2N_H$	0	1	0	$2N_H$	$k \sum Y^2$
$W$	adj (1, 3, 0)	1	0	4	0	4	0
$G$	adj (8, 1, 0)	1	6	0	6	0	0

Note:  $w_1^{(f)} = 12 \sum Y^2$  for Weyl fermions and  $w_1^{(s)} = 3 \sum Y^2$  per hypercharged scalar degree of freedom. For  $H \sim (\mathbf{1}, \mathbf{2}, \frac{1}{2})$ ,  $\sum_{\text{dof}} Y^2 = 1/2$  so  $w_1(H) = 3$ , ensuring all entries in  $\Delta W$  are integers.

Table 9: EW window  $W_{\text{EW}}$  :  $Q \in (80, 160) \text{ GeV}$ . Heavy multiplets removed, narrow threshold masks.

Removed multiplet	Reason	Mask range in $Q$
top quark	decoupled below $W_{\text{EW}}$	—
<i>Within-window threshold masks:</i>		
$W^\pm$	resonance/threshold guard	$Q \in (79, 82) \text{ GeV}$
$Z$	resonance/threshold guard	$Q \in (90, 92.5) \text{ GeV}$
$H$	threshold guard	$Q \in (124, 127) \text{ GeV}$

Table 10: Low GeV window  $W_{\text{SM}}$  :  $Q \in (1, 10) \text{ GeV}$ . Heavy multiplets removed, edge guards near thresholds.

Removed multiplet	Reason	Mask range in $Q$
$t, W/Z/H$	decoupled below EW scale	—
$c, b$ (edges)	onset guards at $m_c, m_b$	small masks around $m_c, m_b$

Table 11: One-loop counterterm container map near equilibrium (finite parts).

Counterterm	Container
$c_1 R^2 + c_2 R_{\mu\nu} R^{\mu\nu}$	finite normalization of EH sector (no PF term)
$d_1 R \Delta \hat{\Xi}^2$	renormalizes $\sigma_\chi$ in the gate expansion
$e_1 \nabla_\mu \hat{\Psi} \mathbf{K}_{\text{eq}} \nabla^\mu \hat{\Psi}$	renormalizes $\mathbf{K}_{\text{eq}}$ (wavefunction)
$e_2 \hat{\Psi}^\top M^2 \hat{\Psi}$	renormalizes $M^2$ in $V(\hat{\Psi})$

Table 12: Threshold mask ranges (excluded from  $F_\sigma$  statistics).

Threshold	Central value [GeV]	Masked range [GeV]
$W$	80.4	[79.0, 82.0]
$Z$	91.2	[90.0, 92.5]
$H$	125.3	[124.0, 127.0]
$t$	172.5	[171.0, 175.0]
$b$	4.18	[4.10, 4.30]
$c$	1.27	[1.20, 1.35]

# GAGE\_repo code pack (copy-safe, ASCII)

Michael DeMasi DNP

---

## Layout

Files printed below (in order):

README.txt; pins.json; src/omega\_chi.py; src/gate\_null.py; src/ward\_flatness\_stub.py (optional); src/snake\_check.py (optional; needs sympy); build.sh; checksums.py

*Usage:* Save each block to the exact filename shown, then run `bash build.sh`. Outputs: results.json, stdout.txt, SHA256SUMS.txt.

## README.txt

```
GAGE_repo (from-scratch, deterministic, ASCII)
```

### Purpose:

Recompute Omega\_chi, alphaG\_pp, closure Omega\_chi/alphaG\_pp, leave-one-out alpha\_s\*(MZ), the lab quadratic null DeltaG/G ~ $\approx (\Delta\chi/\sigma_\chi)^2$ , and the kinetic-metric diagnostics: eigens of K\_eq, ||chi||\_K, alignment cos(theta), and Lambda\_gate.

### Quickstart:

- 1) Save these files as shown (flat folder, keep names).
- 2a) macOS/Linux: bash build.sh
- 2b) Windows (PS): .\build\_win.bat
- 3) Inspect results.json, metric\_results.json, stdout.txt, SHA256SUMS.txt

### Determinism:

- No RNG, no network calls
- All constants pinned in pins.json and keq.json
- Checksums recorded in SHA256SUMS.txt

### Outputs:

- results.json # Omega\_chi, alphaG\_pp, closure, alpha\_s\* (LOO), Lambda\_gate
- metric\_results.json # eigvals/evecs(K\_eq), ||chi||\_K, Lambda\_gate(calc), alignment
- stdout.txt # human-readable summaries (appended)
- SHA256SUMS.txt # SHA-256 over the above artifacts

### Run individually (PowerShell):

```
python src\omega_chi.py
python src\gate_null.py
python src\metric_eigs.py
python src\snf_check.py      # optional, needs sympy
python checksums.py
```

### Optional:

- src/snake\_check.py certifies chi = (16,13,2) via exact integer kernel/SNF (needs sympy)
- src/ward\_flatness\_stub.py wiring for F\_sigma monitor (you add RGE grid later)
- numpy or sympy enables eigen-decomposition in metric\_eigs.py (numpy preferred)

## pins.json

```
{  
    "meta": {  
        "scheme": "MS",  
        "scale": "MZ",  
        "notes": "Hats at MZ in MS; SI pins for alphaG_pp"  
    },  
    "pins": {  
        "alpha_s_MZ": 0.1180,  
        "inv_alpha_MZ": 127.955,  
        "sin2_thetaW_MZ": 0.23129,  
        "G_N_SI": 6.67430e-11,  
        "m_p_SI_kg": 1.67262192369e-27,  
        "hbar_SI_Js": 1.054571817e-34,  
        "c_SI_mps": 299792458.0  
    },  
    "gate": {  
        "sigma_chi": 247.683,  
        "K_eq_norm_chi": 17.6278  
    },  
    "projector": { "chi": [16, 13, 2] }  
}
```

## src/omega\_chi.py

```
#!/usr/bin/env python3  
import json, math, sys, pathlib  
  
def load_pins(path="pins.json"):  
    with open(path,"r") as f: return json.load(f)  
  
def alpha2(alpha_em, sin2w): return alpha_em / sin2w  
def omega_chi(alpha_s, alpha2, alpha_em): return (alpha_s**16)*(alpha2**13)*(alpha_em**2)  
def alpha_G_pp(G_N, m_p, hbar, c): return G_N * (m_p**2) / (hbar * c)  
def loo_alpha_s_star(alpha_Gpp, alpha2, alpha_em):  
    return (alpha_Gpp / (alpha2**13 * alpha_em**2))**(1.0/16.0)  
  
def main():  
    pins = load_pins()  
    P, G = pins["pins"], pins["gate"]  
  
    alpha_em = 1.0 / float(P["inv_alpha_MZ"])  
    sin2w = float(P["sin2_thetaW_MZ"])  
    a_s = float(P["alpha_s_MZ"])  
    a_2 = alpha2(alpha_em, sin2w)  
  
    aGpp = alpha_G_pp(float(P["G_N_SI"]), float(P["m_p_SI_kg"]),  
                      float(P["hbar_SI_Js"]), float(P["c_SI_mps"]))  
    Om = omega_chi(a_s, a_2, alpha_em)  
    closure = Om / aGpp  
    a_s_star = loo_alpha_s_star(aGpp, a_2, alpha_em)
```

```

Lambda_gate = float(G["sigma_chi"]) / float(G["K_eq_norm_chi"])

out = {
    "alpha2_MZ": a_2,
    "Omega_chi": Om,
    "alpha_G_pp": aGpp,
    "closure_ratio_Omega_over_alphaGpp": closure,
    "alpha_s_star_MZ": a_s_star,
    "Lambda_gate": Lambda_gate
}

with open("results.json", "w") as f: json.dump(out, f, indent=2, sort_keys=True)
s = (f"alpha2(MZ) = {a_2:.9f}\n"
      f"Omega_chi = {Om:.12e}\n"
      f"alphaG_pp = {aGpp:.12e}\n"
      f"closure Omega_chi/alphaG_pp = {closure:.8f}\n"
      f"alpha_s* (LO0) = {a_s_star:.9f}\n"
      f"Lambda_gate = {Lambda_gate:.6f}")
print(s)
with open("stdout.txt", "w") as f: f.write(s)

if __name__ == "__main__":
    main()

```

### src/gate\_null.py

```

#!/usr/bin/env python3
import json

def load_gate(path="pins.json"):
    with open(path, "r") as f: j = json.load(f)
    return float(j["gate"]["sigma_chi"]), float(j["gate"]["K_eq_norm_chi"])

def deltaG_over_G_from_phi(phi_chi, sigma_chi, norm_chi_Keq):
    # DeltaXi = ||chi||_K * phi_chi ; DeltaG/G ~= (DeltaXi/sigma_chi)^2 near equilibrium
    dXi = norm_chi_Keq * phi_chi
    return (dXi / sigma_chi)**2

if __name__ == "__main__":
    sigma, norm = load_gate()
    phi = 1.0
    print(f"phi_chi={phi}, DeltaG/G ~= {deltaG_over_G_from_phi(phi, sigma, norm):.6e}")

```

### src/metric\_eigs.py (optional)

```

#!/usr/bin/env python3
# metric_eigs.py -- K_eq eigens, ||chi||_K, alignment, Lambda_gate (ASCII-only)

import json, math
from pathlib import Path

```

```

HERE = Path(__file__).resolve().parent
ROOT = HERE.parent # repo root

def load_json(name):
    # try src/ first, then repo root
    p = HERE / name
    if not p.exists():
        p = ROOT / name
    with open(p, "r") as f:
        return json.load(f)

def is_symmetric(M, tol=1e-12):
    for i in range(3):
        for j in range(3):
            if abs(M[i][j] - M[j][i]) > tol:
                return False
    return True

def matvec(M, v):
    return [sum(M[i][j]*v[j] for j in range(3)) for i in range(3)]

def dot(a, b):
    return sum(x*y for x, y in zip(a, b))

def eigen_decomp_sym(M):
    try:
        import numpy as np
        w, V = np.linalg.eigh(np.array(M, dtype=float))
        evecs = [[V[i, k] for i in range(3)] for k in range(3)]
        return w.tolist(), evecs
    except Exception:
        from sympy import Matrix
        mat = Matrix(M)
        evecs = mat.eigenvecs()
        pairs = []
        for ev, mult, vecs in evecs:
            for v in vecs:
                vv = [float(x) for x in v]
                nrm = math.sqrt(sum(x*x for x in vv))
                if nrm == 0.0:
                    continue
                vv = [x/nrm for x in vv]
                pairs.append((float(ev), vv))
        pairs.sort(key=lambda t: t[0])
        evals = [p[0] for p in pairs]
        evecs = [p[1] for p in pairs]
        return evals, evecs

def main():
    pins = load_json("pins.json")
    chi = [float(x) for x in pins["projector"]["chi"]]
    sigma_chi = float(pins["gate"]["sigma_chi"])
    keq_norm_pin = float(pins["gate"]["K_eq_norm_chi"])

```

```

K = load_json("keq.json")["K_eq"]
if not is_symmetric(K):
    K = [[0.5*(K[i][j] + K[j][i]) for j in range(3)] for i in range(3)]

# K-norm of chi
Kchi = matvec(K, chi)
chi_norm_K = math.sqrt(dot(chi, Kchi))

# Eigenvalues/eigenvectors (ascending)
evals, evecs = eigen_decomp_sym(K)
soft_idx = 0
v_soft = evecs[soft_idx]
nvs = math.sqrt(dot(v_soft, v_soft))
if nvs != 0.0:
    v_soft = [x/nvs for x in v_soft]

# Alignment cosine (Euclidean)
chi_norm = math.sqrt(dot(chi, chi))
cos_theta = abs(dot(chi, v_soft)) / chi_norm if chi_norm != 0.0 else float("nan")

# Gate scale
Lambda_gate_calc = sigma_chi / chi_norm_K
Lambda_gate_pin = sigma_chi / keq_norm_pin if keq_norm_pin != 0.0 else float("inf")

# JSON artifact (repo root)
out = {
    "K_eq": K,
    "eigvals_sorted": evals,
    "soft_index": soft_idx,
    "v_soft": v_soft,
    "chi": chi,
    "chi_norm_K": chi_norm_K,
    "chi_norm_K_pinned": keq_norm_pin,
    "chi_norm_K_diff": chi_norm_K - keq_norm_pin,
    "sigma_chi": sigma_chi,
    "Lambda_gate_calc": Lambda_gate_calc,
    "Lambda_gate_from_pins": Lambda_gate_pin,
    "Lambda_gate_diff": Lambda_gate_calc - Lambda_gate_pin,
    "alignment_cosine": cos_theta
}
with open(ROOT / "metric_results.json", "w", encoding="ascii") as f:
    json.dump(out, f, indent=2, sort_keys=True)

# Human-readable summary (append to stdout.txt in repo root)
s = []
s.append("K_eq eigenvalues (asc): " + ", ".join(f"{x:.7f}" for x in evals))
s.append("Soft-mode eigenvector: (" + ", ".join(f"{x:.7f}" for x in v_soft) + ")")
s.append(f"||chi||_K (computed): {chi_norm_K:.6f}")
s.append(f"||chi||_K (pinned) : {keq_norm_pin:.6f}")
s.append(f"Lambda_gate (calc) : {Lambda_gate_calc:.6f}")
s.append(f"Lambda_gate (pins) : {Lambda_gate_pin:.6f}")
s.append(f"Lambda diff : {Lambda_gate_calc - Lambda_gate_pin:.6e}")
s.append(f"Alignment cos(theta): {cos_theta:.7f}")
txt = "\n".join(s) + "\n"

```

```

print(txt, end="")
with open(ROOT / "stdout.txt", "a", encoding="ascii") as f:
    f.write(txt)

if __name__ == "__main__":
    main()

```

**keq.json (input)** Symmetric positive-definite equilibrium kinetic metric in the  $(\ln \alpha_s, \ln \alpha_2, \ln \alpha)$  basis.

```
{
    "K_eq": [
        [1.2509, -0.6202, -0.1813],
        [-0.6202, 1.5128, -0.1633],
        [-0.1813, -0.1633, 3.2362]
    ],
    "notes": "Equilibrium kinetic metric Keq in (ln alpha_s, ln alpha_2, ln alpha)."
}
```

### src/ward\_flatness\_stub.py (optional)

```

#!/usr/bin/env python3
def betaXi_over_logQ(alpha_s, alpha2, alpha_em, betas):
    # beta_Xi = 16*beta_s/alpha_s + 13*beta_2/alpha_2 + 2*beta_em/alpha
    return 16*betas["beta_s"]/alpha_s + 13*betas["beta_2"]/alpha2 +
        2*betas["beta_em"]/alpha_em

def normalized_F_sigma(betaXi, sigma_chi): return betaXi / sigma_chi

if __name__ == "__main__":
    print("Stub: provide (Q, alpha_s, alpha_2, alpha, betas)
grid and accumulate |F_sigma| stats.")

```

### src/snake\_check.py (optional; needs sympy)

Exact-integer Smith normal form (SNF) + unimodular transport; certificate that  $\chi = (16, 13, 2)$  arises from integer right-kernel of `DeltaW_EM`. *Optional; build passes without SymPy.*

```

#!/usr/bin/env python3
# snf_check.py -- exact-integer SNF + primitive kernel for DeltaW_EM (version-robust)

from sympy import Matrix, ilcm, igcd, ZZ

# Define the DeltaW_EM matrix in the (SU3, SU2, EM) basis
A = Matrix([[8, 224],
            [0, 18]])  # DeltaW_EM

U = D = V = None

# 1) Try Matrix method (newer SymPy)

```

```

if hasattr(Matrix([[1]]), "smith_normal_form"):
    try:
        U, D, V = A.smith_normal_form() # U*A*V = D
    except Exception:
        U = D = V = None

# 2) Fallback: module function (older SymPy), normalize return signatures
if D is None:
    try:
        from sympy.matrices.normalforms import smith_normal_form as snf_func
        try:
            out = snf_func(A, domain=ZZ, calc_transform=True)
        except TypeError:
            out = snf_func(A, domain=ZZ)

        # Normalize various return signatures
        if isinstance(out, tuple):
            if len(out) == 3: # could be (D,U,V) or (U,D,V)
                for Dm, Um, Vm in [(out[0], out[1], out[2]),
                                     (out[1], out[0], out[2]),
                                     (out[2], out[0], out[1])]:
                    try:
                        if Um*A*Vm == Dm:
                            D, U, V = Dm, Um, Vm
                            break
                    except Exception:
                        pass
            elif len(out) == 2 and isinstance(out[1], tuple) and len(out[1]) == 2:
                D, (U, V) = out
            else:
                D = out # D only
        except Exception:
            pass

    # --- Validate SNF if available ---
    m, n = A.shape
    if D is not None:
        assert D.shape == (m, n)
        # rank = number of nonzero diagonal entries
        r = sum(1 for i in range(min(m, n)) if D[i, i] != 0)
        assert r == 2, f"Expected rank 2; got {r}"
        # columns beyond rank must be all zeros (here: the 3rd column)
        for j in range(r, n):
            assert all(D[i, j] == 0 for i in range(m)), "Trailing column not zero in D"
    else:
        r = 2 # expected for this A; continue without D/U/V assertions

    # --- Kernel from SNF if V present (preferred) ---
    chiZ_snf = None
    if V is not None and D is not None:
        chiZ_snf = V[:, -1] # last column spans ker_Z(A) since n - r = 1
        if chiZ_snf[-1] < 0:
            chiZ_snf = -chiZ_snf

```

```

# --- Fallback: rational nullspace, integerize, primitive ---
chiQ = A.nullspace()[0]           # rational kernel
den = 1
for q in chiQ:
    den = ilcm(den, getattr(q, 'q', 1))   # LCM of denominators
chiZ_rat = den * chiQ             # integer entries now
g = abs(int(igcd(*[int(v) for v in chiZ_rat])))
chiZ_rat = chiZ_rat.applyfunc(lambda v: v // g)  # elementwise integer divide
if chiZ_rat[-1] < 0:
    chiZ_rat = -chiZ_rat

# Choose kernel (prefer SNF path if available)
chiZ = chiZ_snf if chiZ_snf is not None else chiZ_rat

# Checks
assert A*chiZ == Matrix([0, 0])
assert tuple(chiZ) == (-10, -18, 1)  # EM-basis primitive kernel

# Unimodular transport to (alpha_s, alpha_2, alpha)
M = Matrix([[ -5, -3, -2],
            [  2,  1,  1],
            [  2,  1,  0]])
assert M.det() in (1, -1)
chi_gauge = M.T * chiZ
assert tuple(chi_gauge) == (16, 13, 2)

# Report
if D is not None:
    diag_list = [D[i, i] for i in range(min(m, n)) if D[i, i] != 0]
    print("SNF invariant factors (diagonal):", diag_list)  # expected [1, 8]
else:
    print("SNF transform matrices not available in this SymPy build; used rational nullspace path.")
print("Primitive kernel in (SU3,SU2,EM):", tuple(chiZ))
print("Transported kernel in (alpha_s, alpha_2, alpha):", tuple(chi_gauge))
print("All checks passed.")

```

## build.sh

```

#!/usr/bin/env bash
set -euo pipefail
mkdir -p src

python3 src/omega_chi.py | tee /dev/stderr
python3 src/gate_null.py | tee -a /dev/stderr

# Optional checks (won't fail the build)
python3 src/ward_flatness_stub.py || true
python3 -c "import sympy" >/dev/null 2>&1 && python3 src/snf_check.py || true

python3 checksums.py
echo "OK"

```

## checksums.py

```
#!/usr/bin/env python3
import hashlib, os

def sha256(p):
    h = hashlib.sha256()
    with open(p,'rb') as f:
        for chunk in iter(lambda: f.read(8192), b''):
            h.update(chunk)
    return h.hexdigest()

def main():
    outs = [p for p in ["results.json","stdout.txt"] if os.path.exists(p)]
    with open("SHA256SUMS.txt","w") as f:
        for p in outs:
            s = f"sha256({p}) {p}"
            print(s)
            f.write(s+"\n")

if __name__ == "__main__":
    main()
```